Journal of Materials Chemistry B

ROYAL SOCIETY OF CHEMISTRY

REVIEW

View Article Online
View Journal | View Issue

Cite this: J. Mater. Chem. B, 2023, 11, 5272

Progress in the preparation of Prussian blue-based nanomaterials for biomedical applications

Kun Lu,[a] Xiao-Yang Zhu,[a] Yan Li *[a] and Ning Gu *[ab]

Received 30th November 2022,
Accepted 19th January 2023

DOI: 10.1039/d2tb02617a

rsc.li/materials-b

Prussian blue (PB) is composed of the coordination network of Fe^{2+}–C≡N–Fe^{3+} mixed valence state as a classic metal complex, which includes a C atom and Fe^{2+} (low spin), N atom and Fe^{3+} (high spin). PB and its analogues (PBA) have excellent biosafety, good magnetic properties, outstanding photothermal properties and the ability to mimic enzymatic behaviors due to their stable structure, tunable size, controllable morphology, abundant modification methods and excellent physicochemical properties. They have received increasing research interest and have shown promising applications in the biomedical field. Here, progress in the preparation of PB-based nanomaterials for biomedical applications is summarized and discussed. The preparation strategies, traditional synthesis and emerging preparation methods of PB are summarized systematically in this review. The design and preparation of PBA, PB(PBA)-based hollow structures and PB(PBA)-based composites are also included. While introducing the preparation status, some PB-based nanomaterials that have performed well in specific biomedical fields are emphasized. More importantly, the key factors and future development of PB for the clinical translation as multifunctional nanomaterials are also discussed. This review provides a reference for the design and biomedical application of PB-based nanomaterials.

10th anniversary statement

For the 10th anniversary of JMCB, we would like to express our warm congratulations and heartfelt thanks to you! In the past ten years, JMCB has focused on excavating and reporting high-quality research results in the field of biomaterials, leading emerging research directions in materials chemistry, and creating a journal with a unique style that is popular with researchers. JMCB focuses on the new understanding, application, performance and synthesis of materials, it has become an important international academic platform and the pioneer of academic journals. With the approval and help of the editorial department and reviewers, our research group published several papers on iron-based nanomaterials on JMCB. In the future, we will continue to explore more related research and hope to be recognized and supported by JMCB.

It's our pleasure to celebrate this important moment with you. At this time of celebration, we hope that JMC will innovate and develop characteristically and continue to serve as a display platform for innovative research on materials chemistry in the new journey.

[a] State Key Laboratory of Bioelectronics, Jiangsu Key Laboratory for Biomaterials and Devices, School of Biological Science and Medical Engineering, Southeast University, Nanjing 210009, P. R. China. E-mail: liyan@seu.edu.cn, guning@seu.edu.cn

[b] Medical School, Nanjing University, Nanjing 210093, P. R. China

Kun Lu

Kun Lu is currently a doctoral candidate in Biomedical Engineering at Southeast University. He received his Master's degree in Polymer Chemistry and Physics from Changchun University of Technology in 2020. His research includes the design, synthesis and biomedical applications of Prussian blue nanoparticles.

Xiao-Yang Zhu

Xiaoyang Zhu is currently a Master's candidate in Biomedical Engineering at Southeast University. She received her Bachelor's degree in Biomedical Engineering from Southeast University in 2019. Her current research interest is the combination of artificial intelligence and nanotechnology science.

1. Introduction

Prussian Blue (PB) was first discovered in the 18th century and was originally used as a pigment. The chemical formula of PB is $Fe_4[Fe(CN)_6]_3$, and its structure consists of a mixed valence hexacyanoferrate of Fe^{2+} and Fe^{3+}. The low-spin Fe^{2+} is connected to C atoms, and the high-spin Fe^{3+} is connected to an N atom in the structure of PB. Each Fe^{2+}–C≡N–Fe^{3+} structural unit has five unpaired electrons, and there are redundant Fe^{3+} sites in the PB structure, which can be multifunctionally modified. With the development of technology and research exploration, PB has been widely used in many fields after in-depth research on its chemical structure, synthesis method and application direction. Due to the simple and abundant preparation method and controllable size of PB, it has been widely used in supercapacitors,[1,2] sensors,[3] catalysis,[4] gas storage,[5–7] photothermal therapy,[8] medical imaging,[9] drug delivery,[10] nanoenzymes[11] and other fields with good applications. Effective research progress and outstanding application progress have been made in the above-mentioned directions. Due to the reliable biosafety of PB, the clinical application has been approved by the FDA (Food and Drug Administration). Furthermore, with the development of diagnostic and treatment techniques and nanotechnology, PB is a material with great development potential in the field of biomedicine, and many biomedical researchers continue to conduct extensive research on it. Medical diagnosis is mainly divided into three forms, namely laboratory analysis method, medical imaging method, and biosensor method. The research and innovation of contrast agents have important clinical significance since medical imaging is an important means of visual monitoring and disease diagnosis. Due to the improved performance requirements and the ever-changing medical diagnostic methods of contrast agents, nanotechnology has played an important role in the preparation and application of diagnostic materials used in clinical applications. PB and Prussian blue analogs (PBAs) usually have excellent magnetic properties, and the controllability and particularity of their structures also endow them with good optical properties. Thus, they can be used as contrast agents for magnetic resonance imaging, photoacoustic imaging, and ultrasound imaging.[12,13] Drug delivery systems provide new avenues for drug transport and controlled release. Metal–organic frameworks (MOFs) are organic–inorganic hybrid materials with intramolecular pores formed by the self-assembly of organic ligands and metal ions or clusters through coordination bonds, and are often used as drug carriers in biomedical applications. PB, as a material with a special structure in MOFs, is often selected as a drug carrier because of its porosity and large specific surface area. It endows the material with a good drug loading rate. Due to the redundant Fe^{3+} sites in PB, electrostatic interactions can be performed to improve drug loading rates, and modifications can be made to achieve targeted release. At the same time, as a drug carrier, the structural stability of PB is also much greater than that of other MOF materials, so it can control and release drugs more effectively.[14,15] Moreover, PB, as an iron-containing nano-mimetic enzyme, has a typical Fenton effect or electron transfer mechanism. This makes it have excellent multi-type enzyme activities, including the inhibition of tumor growths and metastasis, and achieving therapeutic effects.[16,17] Photothermal therapy is a new cancer treatment method that has emerged in recent years.[18] In general, the traditional photothermal nanomaterials are mainly gold nanoparticles,[19] silver nanoparticles,[20] carbon nanoparticles,[21] platinum nanoparticles[22] and their derivatives.[23] However, traditional photothermal nanomaterials often have the disadvantages of large required photothermal conversion area, poor near-infrared conversion rate, and high price. Therefore, the development of photothermal nanomaterials with simple preparation, good photothermal performance, good biocompatibility and diversified functions has become a research hotspot. As a representative of organic dyes used as photothermal agents, PB is in the research upsurge for its excellent photothermal conversion efficiency, green low-cost synthesis and excellent biosafety rate.[24] PB, as a photothermal agent, can also play a role

Yan Li

Yan Li is currently an Associate Professor of Biomedical Engineering at Southeast University. She received her PhD degree in Materials Science and Engineering from Tsinghua University in 2008. Her research includes the design and construction of biomaterials, the interactions between cells and biomaterials, and the biomedical applications of stem cells.

Ning Gu

Ning Gu is currently a Professor at Nanjing University. He received his PhD degree in Biomedical Engineering from Southeast University in 1996. Prior to joining Nanjing University, he was a Professor at Southeast University. Among other awards, he has obtained the Cheung Kong Scholars Programme of the Ministry of Education of China and the National Science Fund for Distinguished Young Scientists of China. He is an academician of the Chinese Academy of Sciences, a fellow of the Chinese Society of Micro-Nano Technology, and a fellow of the American Academy of Medical and Biological Engineering. His main scientific interest is focused on biomedical nanomaterials.

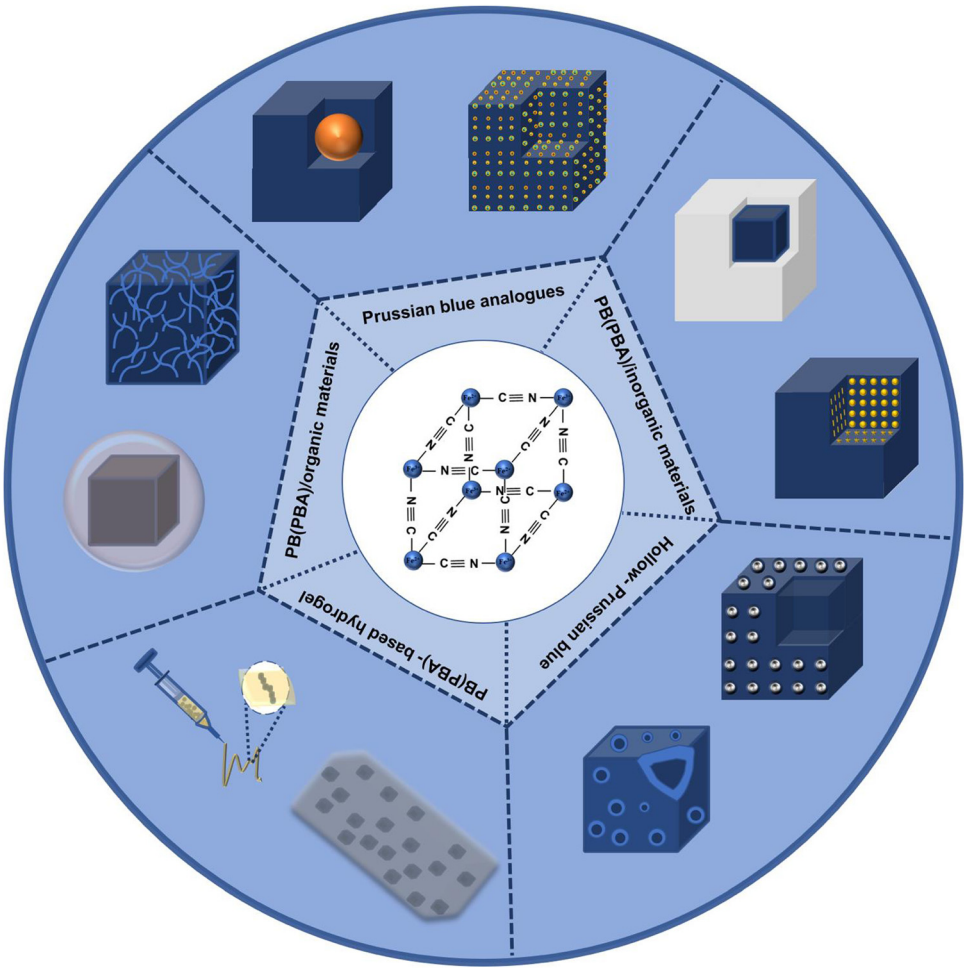

Fig. 1 Scheme of Prussian blue, Prussian blue analog, Prussian blue composite nanomaterials and Prussian blue compound.

as a contrast agent and nanozyme to achieve the effect of integrated diagnosis and treatment. In short, PB and PBA exhibit excellent biomaterial properties from diagnosis to therapy.

With the gradual deepening of PB research, the simple structure has been unable to meet the growing application needs, while optimizing the preparation process. Furthermore, some PBA or Prussian blue composite nanomaterials were gradually designed and developed, as shown in Fig. 1. By replacing the iron element in the PB framework with other transition metals, and controlling the valence state of the transition metals, or changing the interstitial ions in the framework, a series of complexes similar in structure and properties to PB can be obtained. Herein, this article introduces the status and prospects of PB and PBA as biological materials, and mainly introduces their synthetic methods and research potential.

2. Synthetic strategies and synthetic methods of Prussian blue

2.1 Synthetic strategies of PB

In general, the material's synthesis process and preparation technologies play a significant role in whether the material may be used. The process of preparing PB has received a lot of attention since it has the potential to be used in a variety of disciplines, particularly as a biomedical material. In terms of the synthesis strategy, the preparation strategies for PB can be separated into dual-precursor synthesis and single-precursor synthesis. As shown in Fig. 2, the principle of the dual-precursor synthesis strategy is that a solution of Fe^{2+} or Fe^{3+} with equimolar iron content and $[Fe(CN)_6]^{3-}$ or $[Fe(CN)_6]^{4-}$ under specific conditions are mixed to form PB. For example, by combining Fe^{2+}, $[Fe(CN)_6]^{3-}$, and PVP dissolved in water, Kitagawa *et al.* were able to produce PVP-protected PB with good dispersibility.[25] In a single-precursor synthesis, $K_3[Fe(CN)_6]$ or $K_4[Fe(CN)_6]$ or other monomers are used as the only iron supply. These monomers will be reduced to Fe^{2+} or Fe^{3+} by a reducing agent, and the reduced iron ions will then quickly react with the precursor to create PB. The excellent monodispersity of the NPs produced by the slow reaction processes makes this approach an ideal one for producing PBNPs. Jia *et al.* selected $Fe_4[Fe(CN)_6]_3$ as a single precursor to prepare PB, and adjusted the crystallinity and analyzed the effect on the potential of nanoparticles by adjusting the temperature and the concentration of the precursor.[26] Under the same strategy, Li *et al.* added $[Fe(CN)_6]^{3-}$ to the pH-adjusted chitosan solution, and then

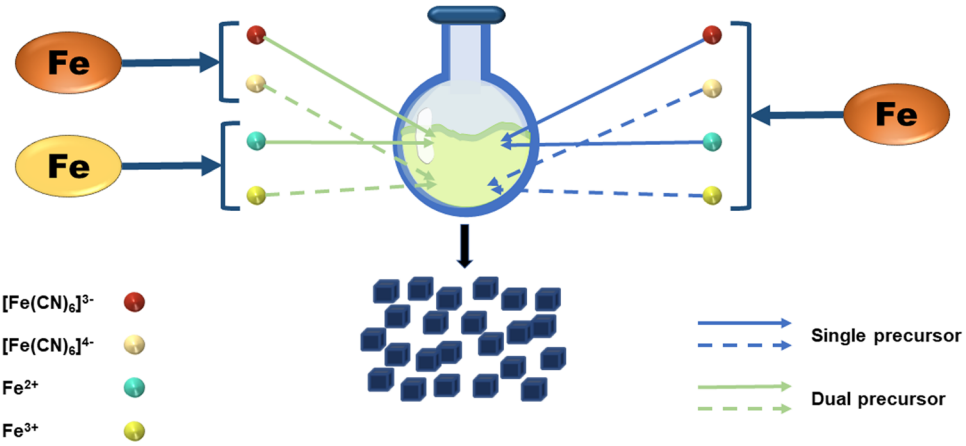

Fig. 2 Schematic of the synthetic strategy of Prussian blue.

slowly added the $FeCl_2$ solution dropwise with vigorous stirring. The solution then darkened to form a chitosan-PB composite material.[27] After modification, the size of nanoparticles can be controlled to a certain extent, and chitosan can also be further modified to achieve better applications. A single iron source can also regulate the size of PBNPs by regulating the concentration of other substances in the reaction system. $K_4[Fe(CN)_6]$ was used as a single precursor in the modified hydrothermal technique used by Cai *et al.* to created PBzyme with a particle size of 65 nm.[28] The work demonstrated that PBNPs suppress inflammation by modulating the PPAR-γ/NF-κB signaling pathway. In terms of the preparation process, the single-precursor preparation method is not only simple and controllable in reactants and reaction conditions, but it is also more convenient to operate in specific implementation steps than dual-precursor preparation. This further demonstrates the advantages of single-precursor preparation. In recent studies, the dual precursor method has often been used to introduce other elements into the PB framework to form PBA, which will be introduced in the following sections.

2.2 Synthetic methods of PB

2.2.1 Preparation of PB by coprecipitation. The preparation of nanoparticles by co-precipitation usually refers to the nucleation, growth, ripening and final precipitation of two or more ions in the reaction solution or precipitant during the reaction process.[29–33] The nanoparticles that are produced typically have good dispersion and uniformity due to the relatively constant ratio of each component in the reaction. Most of the time, co-precipitation is broken down into single-phase co-precipitation and mixed-phase co-precipitation, which also represent the two PBNPs synthesis strategies (single-precursor and dual-precursor, respectively). The following factors typically influence the coprecipitation of the PB preparation: the reaction temperature, the PBNPs' crystallinity, and the material-to-product ratio. These three factors determine whether the reaction can proceed. The co-precipitation method is PB's most fundamental and straightforward synthesis method. The initial co-precipitation preparation method is also continuously improved as new PB applications are discovered. Okawa *et al.* used ascorbic acid as a nucleating agent under the action of a reducing agent of citric acid to tune the size of the dispersed PBNPs by controlling forced nucleation.[34] Congruously, Mohammadreza Shokouhimehr *et al.* also selected citric acid as a surface protective agent to prepare 10–100 nm PB by co-precipitation method as a T_1-weighted magnetic resonance contrast agent. At the same time, it can bond fluorescent molecules on its surface for dual imaging of magnetic resonance and fluorescence,[35] pioneering a new application of PB in the field of medical imaging. On the other hand, PBNPs have a good molar extinction coefficient, photothermal conversion performance, and photothermal stability performance. Due to the strong tissue penetration of near-infrared light, PBNPs convert light energy into heat energy after absorbing near-infrared light. This allows for instantaneous thermoelastic expansion to be detected by an ultrasonic detector, resulting in a photoacoustic imaging picture. In optical imaging, some fluorescent probes can improve the signal-to-noise ratio of the region, thereby improving the detection sensitivity and diagnostic accuracy. The hollow structure of PBNPs can also be used as loaded fluorescent probes to enhance the effect of photoacoustic imaging. Long *et al.* prepared 25 different crystal forms of PB by co-precipitation by selecting $FeCl_3{\cdot}nH_2O$ + $K_4[Fe(CN)_6]{\cdot}3H_2O$ or $FeCl_2{\cdot}4H_2O$ + $K_3[Fe(CN)_6]{\cdot}3H_2O$.[36] At the same time, it was found that the PB crystal growth rate is the best method to improve the quality of the PB pigment and reduce the fading performance. The initial co-precipitation preparation method is also continuously improved as PB application research continues. Meanwhile, it is a good choice to use dual precursors to prepare PBA by co-precipitation method. In recent years, coprecipitation method has been used to prepared PBA to introduce other elements, which could improve the special properties of nanoparticles. In addition, the ideal method has shifted away from the fundamental co-precipitation preparation mechanism, and toward external field-assisted crystallization, growth process control, and other methods to make the co-precipitation method product better. These methods will be introduced in later chapters.

2.2.2 Preparation of PB by microemulsion method. In the microemulsion method, the aqueous and oil phases, when an

emulsifier is present, form droplets of water-in-oil (W/O), oil-in-water (O/W), or multiple microemulsions (O/W/O or W/O/W) in the reaction system as a microreactor.[37–39] Nanoparticles nucleate, grow, aggregate, and ripen in droplets to precisely control the shape and size of the droplets. In the microemulsion preparation method of PB, its emulsifiers are conventionally cetyltrimethylammonium bromide (CTAB), sodium dodecylbenzenesulfonate (SDS), and hexadecane. Alcohol is usually selected for biological safety class as a co-emulsifier. The Wang research group first proposed the miniemulsion periphery polymerization (MEPP) method to prepare hollow PB nanoparticle shells by using the microemulsion method.[40] In the reaction system, toluene was used as an oil phase, hexadecane as an emulsifier, and ferrate was used as a triblock copolymer in the rubber, which reacted on the surface of the micelle. Finally, PB nanoshells with hollow and rigid shells were obtained (Fig. 3A). Next, Wang *et al.* used microemulsion polymerization to prepare hollow PBNPs outside the micelles (Fig. 3B), using toluene as the solvent and poly(ethylene glycol)-*b*-poly(propylene glycol)-*b*-poly(ethylene glycol) as the emulsifier.[41] The pentacyano(4-(dimethylamino)pyridine)-ferrate (Fe-DMAP) groups were attached to the hydrophilic PEO segment. The study was conducive to the more precise preparation of hollow PBNPs to enhance the loading rate. Subsequently, they improved the MEPP synthesis process, adding EPE-DMAP to promote coordination polymerization by binding to the Fe^{3+} moiety from the aqueous phase. Thus, it could be immobilized on the periphery of the oil droplets.[42] The results show that when Fe^{3+} is added to the mini-emulsion, when the ratio of EPE-Fe : EPE-DMAP (or EPE-OH) is 60 : 40 (w/w), metal coordination polymerization will occur to form nanocubes (Fig. 3C). The research further showed that the synthesis site is an important reason for the formation of specific nanoparticle structures (Fig. 3D). In a separate study, Liu *et al.* chose Triton X-100 as the emulsifier.[8] The same mass ratio of hexanol and cyclohexane were added into a tube and stirred at room temperature. After stirring to form an emulsion, a certain amount of $K_3[Fe(CN)_6]$ aqueous solution and citric acid were prepared. After mixing uniformly, it was heated to the reaction temperature of 80 °C. Finally, PBNPs of 20–30 nm were obtained for photothermal therapy of VX2 tumors in rabbits (Fig. 3E and F). In general, the microemulsion preparation method can control the size of PBNPs more efficiently through emulsion microspheres. However, because of the use of surfactants, it often requires a large amount of solvent washing. This increases the difficulty of purification and complicates the preparation process, which is not conducive to large-scale preparation. Therefore, emulsifiers with excellent biocompatibility will become the key to the preparation of PBNPs.

2.2.3 Preparation of PB by hydrothermal method. The hydrothermal method is carried out in a specific closed reactor, such as a high temperature and pressure reactor. The reaction is controlled by the reaction temperature, the concentration of the reactants, and the reaction time. In recent years, many studies have proposed a low-temperature and low-pressure hydrothermal method for the synthesis of inorganic nanoparticles to simplify the preparation process.[43–46] The hydrothermal method of PB is

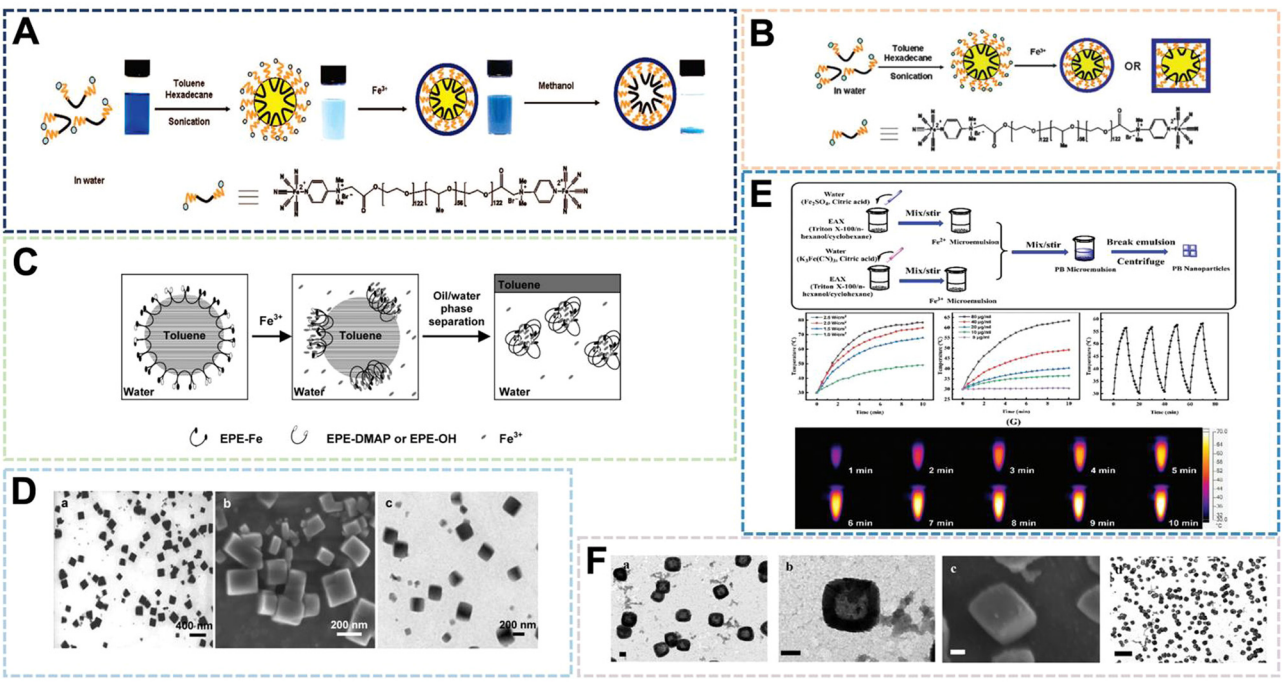

Fig. 3 (A)–(C) Schematic Illumination of PB nanoshells Produced through MiniEmulsion Periphery Polymerization (MEPP). Reprinted from ref. 40 with permission. Copyright 2009 American Chemical Society. Reprinted from ref. 41 with permission. Copyright 2010 Royal Society of Chemistry. Reprinted from ref. 42 with permission. Copyright 2010 Wiley. (D) PBNPs prepared by MEPP method. Reprinted from ref. 42 with permission. Copyright 2010 Wiley. (E) Photothermal properties of PBNPs prepared by microemulsion method. Reprinted from ref. 8 with permission. 2021 Royal Society of Chemistry. (F) PBNPs prepared by microemulsion method. Reprinted from ref. 8 with permission. 2021 Royal Society of Chemistry.

usually prepared by selecting a precursor, a reducing agent or a dispersing agent, and hydrochloric acid, then using water as a solvent, and using a water bath at high temperature and high pressure or low-temperature and low-pressure. Kitagawa *et al.* successfully prepared PBNPs with a size in the range of 10–30 nm by a hydrothermal method with equimolar amounts of $FeCl_2$ and $K_3Fe(CN)_6$ using PVP as a dispersant, in which a part of the amide in the PVP was combined with the external iron ions, providing steric stability to nanoparticles.[25] Under the same conditions, the size of PBNPs prepared without PVP was above 300 nm, and the particle size decreased with the increase of PVP when the iron ion concentration in the reactants was constant. This should be because PVP is coated on the outside of PBNPs, which limits the growth of crystals to a certain extent. At the same time, PVP can also be stably dispersed in several different organic solvents. Dong *et al.* selected $FeCl_3$, $K_3Fe(CN)_6$ and PEI by hydrothermal method, in which $[Fe(CN)_6]^{3-}$ was reduced by PEI to $[Fe((CN))_6]^{4-}$ and Fe^{3+} reacted to form PEI with uniform size distribution protected PBNPs (Fig. 4A). The PEI not only acted as a reducing agent in mechanism, but also better adsorbed on the surface due to electrostatic effect and the coordination effect of the amino group and iron ion.[47] The paper also analyzed the effect of PEI protonation on the formation of PBNPs under different pH values, but did not further explore the Fe^{3+} hydrolysis and hydrolysis products in the system, and this part needs further development. The hydrothermal method is often used in combination with other methods because of its simple reaction composition and convenient preparation process. For example, He *et al.* applied the hydrothermal method to use glucose as a reducing agent and template to prepare highly crystalline PB nanosheets for the first time. The concentration of glucose and the reaction temperature played a crucial role in the size, morphology and composition of the obtained nanoparticles.[48] At the reaction temperature of 100 °C, a cubic morphology was exhibited. When the temperature was increased to 120 °C and 160 °C, PB nanosheets appeared, and the size increased at 160 °C. At 140 °C, the appearance of "nano snowflakes" was also observed (Fig. 4Ba–c). Because $C_6H_{12}O_6$ can also be used as a template for the synthesis of PB nanosheets, $C_6H_{12}O_6$ can be adsorbed on the surface of PB particles through the hydrogen band, thereby minimizing the surface energy (Fig. 4Bd–f). When the growth unit falls on the crystal plane of the PB crystal composed of the (1 0 0) or (0 1 0) plane, the $C_6H_{12}O_6$ surrounding the plane will be desorbed. In turn, the surface energy difference between the exposed (1 0 0) or (0 1 0) facet and other exposed faces of the PB particles increases further, resulting in the oriented growth of PB crystals along the (1 0 0) or (0 1 0) crystal plane direction. Selecting ethanol as the solvent in the preparation process also provides a certain theoretical basis

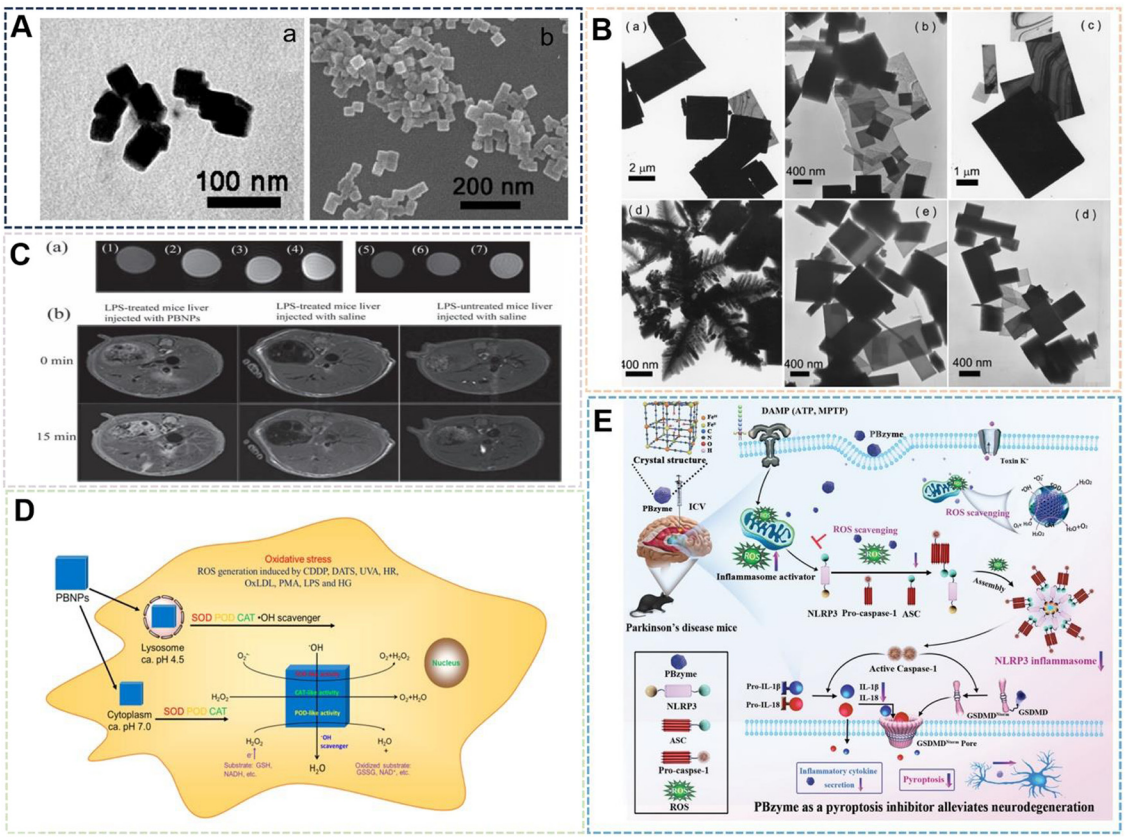

Fig. 4 (A) PBNPs prepared by hydrothermal method. Reprinted from ref. 47 with permission. Copyright 2008 American Chemical Society. (B) PB nanosheets prepared by hydrothermal method. Reprinted from ref. 48 with permission. Copyright 2009 Elsevier. (C) Photoacoustic imaging of PBNPs. Reprinted from ref. 49 with permission. Copyright 2012 Wiley. (D) PBNPs-like enzyme activity. Reprinted from ref. 50 with permission. Copyright 2016 American Chemical Society. (E) ROS scavenging properties of PBNPs. Reprinted from ref. 11 with permission. Copyright 2022 Wiley.

for the solvent method. Since no other solvent is added in the hydrothermal method, the final product can be used after simple purification, which also gives the PBNPs prepared by the hydrothermal method a great space for biological applications. Due to the gradual improvement of the hydrothermal preparation process of PB and the stable preparation of products, many researchers use the hydrothermal as a research basis to explore the biological properties. Nanozyme is a new generation of artificial enzymes based on nanomaterials with simulated enzyme effect, which has high catalytic activity and good stability *in vivo*. The unique properties, such as low preparation cost, have become an indispensable link between nanomaterials and medical technology, which has attracted a large number of researchers to continuously study the design, preparation, mechanism and application of nanoenzyme materials. Through PBNPs prepared by hydrothermal method, we first proposed the CAT-like activity of PBNPs, using it to catalyze the production of O_2 from H_2O_2 in the hepatitis site of mice, and at the same time using ultrasonic microbubbles to perform photoacoustic imaging of the inflammatory site[49] (Fig. 4C). ROS is an intermediate signaling molecule or a direct inducing molecule in most diseases, and it can act as a central regulator of inflammatory signaling. Another most important property of PBNPs as nanozymes is their ability to scavenge ROS, which can effectively reduce inflammation within a certain range the existence of factors. Subsequently, our group for the first time demonstrated that the multi-enzyme activity of PBNPs is caused by the abundant redox potentials of different forms.[50] The work demonstrates the ability of PBNPs to mimic POD, CAT, and SOD, and the results confirm the ability to scavenge ROS in several cellular models (Fig. 4D). However, the detailed cellular mechanisms underlying this property of PBNPs remain unclear. With the gradual discovery of the multi-enzyme activity of PB, the application of its mimetic enzyme activity has also been gradually studied. Zheng *et al.* also chose $K_3[Fe(CN)_6]\cdot 3H_2O$ and PVP, adjusting the pH value with HCl, and reacted the mixture for 20 h to prepare PBNPs by hydrothermal method.[11] Harnessing the activity of the PBNPs nanozymes, the excellent ROS scavenging properties and catalytic activity, inhibited the activation of the microglia NLRP3 inflammasome, thereby reducing neuroinflammation in MPTP-induced PD mice and cellular models (Fig. 4E).

The advantage of the hydrothermal method is that in the reaction system with water as the medium, the reaction rate will be greatly improved, the reaction conditions are simple, and the preparation cost is low. The reaction components of the hydrothermal method are simplified and the preparation process is simple, so it is often combined with other methods, and usually some water-soluble polymer materials such as polysaccharides are often modified and functionalized by the hydrothermal method for PBNPs. This part of the content will be described in detail in the next chapter of this article. The limitation of the hydrothermal method is that the selected reducing agent or dispersant must be water-soluble, which also limits the modification of PBNPs by some poorly water-soluble molecules, so the solvent method has been developed.

2.2.4 Preparation of PB by template-assisted method. The template method is a very important technique for the synthesis of nanomaterials, such as nanowires, nanowires, nanotubes and sheet nanomaterials. The use of the template method to prepare nanomaterials is mainly through the use of template compounds to effectively design and modulate the size, morphology, and arrangement of synthetic materials by using their spatial confinement and structure orientation.[51–54] There are usually two types of templates when using the template method to prepare PBNPs. One is a soft template represented by macromolecules or polymer compounds.[55] Such materials currently mainly form microspheres or micelles to control the growth of PB with the regulation of structural orientation and reduction sites. Dominguez-Vera *et al.* chose apoferritin as a template to synthesize PBNPs.[56] First, they prepared a solution of protein and $[Fe(CN)_6]^{4-}$, and apoferritin dissociated into subunits at pH 2. At pH 8.5, the protein was then reconstituted and Fe^{2+} was added to form PBNPs with a size of around 60 nm (Fig. 5A). However, the mechanism of the material used in its preparation needs to be further verified, especially the existence of PB in apoferritin. Wu *et al.* selected poly(4-vinylpyridine)/polystyrene(P4VP/PS) polymer nanoparticles as templates, in which the P4VP pyridyl moiety could react with $Na_3[Fe(CN)_5HN_3]$ through ligand exchange reaction, and finally added $FeCl_3$ solution formation of PB-coated polymer nanoparticles.[57] In the work, polymers are used as templates, and then the size of the templates can be controlled by polymerization reaction to further control the size, which enriches the synthesis diversity of organic–inorganic hybrid nanoparticles composed of PBNPs. Shen *et al.* used the prepared silver nanospheres and silver nanowires as sacrificial templates to prepare PB nanotubes and hollow PB nanospheres.[58] The outer diameter of the PB nanotubes is about 80 nm, and the wall thickness is about 15 nm (Fig. 5B). Most of the nanotubes in the paper are closed at both ends, and the nanotubes can be broken by ultrasonic action to see the hollow structure. If the two ends can be further controlled so that the ends are not closed during the synthesis process, such an open structure is more conducive to loading. The structure of drugs or other functional nanoparticles will further expand the application scope of PB nanotubes. In recent years, with the demand for size, structure and biosafety of PB as a biological material, and the continuous optimization of preparation technology, the soft template method is usually used in combination with emulsion polymerization. Cai *et al.* prepared HMNPs by emulsion polymerization using polystyrene (PS) nanoparticles, using a mixed micelle concentration (HMC) as a template to prepare hollow PBNPs with HMC as the core and PB as the nanoshell size of 130 nm.[59] At the same time, the study is the first to use 1-pentadecanol (Pent), an FDA-approved biocompatible phase change material, as a controlled release ''drug control valve'' that can respond to elevated temperature by implementing a temperature response feed. The designed PCM-filled hollow magnetic PB nanoparticles are used as novel theranostic drug carriers, and can simultaneously perform MRI, ITI and PAI trimodal imaging (Fig. 5C). As a classic metal–organic framework, PB is also an excellent hard template, and most of the nanoparticles prepared with it as a template have excellent photothermal properties. The preparation

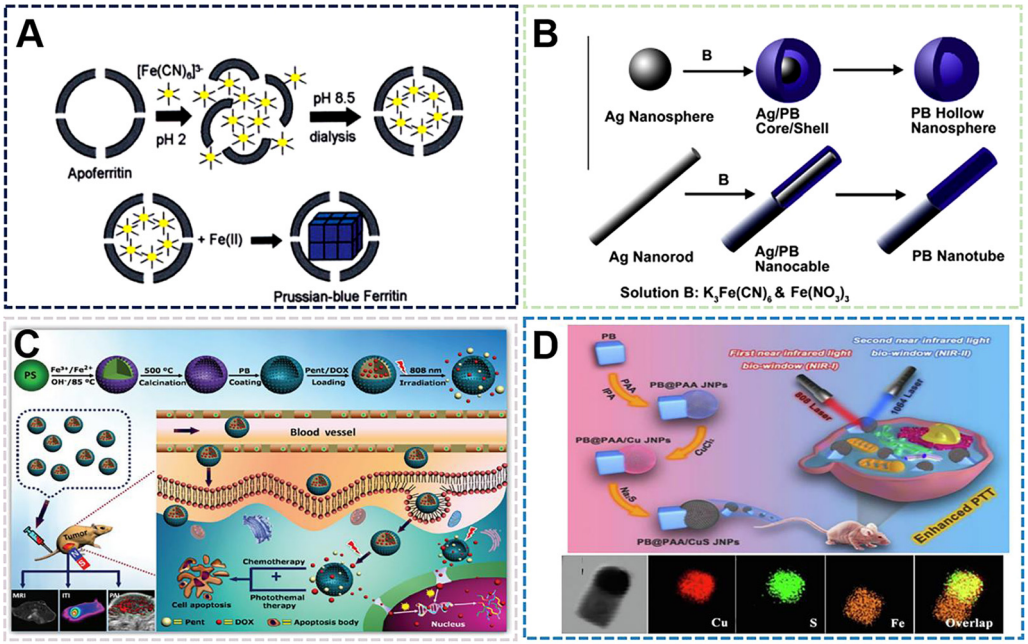

Fig. 5 (A) PBNPs by Apoferritin as a template. Reprinted from ref. 56 with permission. Copyright 2003 American Chemical Society. (B) PBNPs by silver nanospheres and silver nanowires as a template. Reprinted from ref. 58 with permission. Copyright 2014 Elsevier. (C) PBNPs by polystyrene as a template. Reprinted from ref. 59 with permission. Copyright 2017 Wiley. (D) PBNPs by CuS as a template. Reprinted from ref. 60 with permission. Copyright 2022 Elsevier.

technology of composite nanomaterials is constantly updated, and Janus NPs (JNPs) have also been proposed for biomedicine in recent years. Briefly, JNPs are structurally asymmetric and consist of fragments with different compositions, physical, chemical, and surface properties. The other is to use other inorganic materials as hard templates, usually by *in situ* growth of PB on the surface of the template. For instance, Dong *et al.* first prepared PBNPs with a size of about 100 nm by a classical hydrothermal method, and then selectively adsorbed PAA on one surface by utilizing the different diffusion coefficients of the solution system.[60] Finally, Cu^{2+} and S^{2-} were sequentially added to PAA as a template to grow CuSNPs *in situ* in PAA to form CuS/PB@PAA JNPs (Fig. 5D). The preparation technology successfully combines PBNPs with CuSNPs by using a template, and its special Janus structure effectively improves the photothermal conversion efficiency. The nanoparticles exhibited efficient photothermal conversion through the combination of PB and CuS. However, nanoparticles prepared with PB as a template tend to reduce their magnetic and enzymatic activities.

The hard template provides static channels, usually with a certain rigidity, and the reactive species can only enter the channel from the opening or grow on the surface of the template. The soft template provides a cavity in dynamic equilibrium, and substances can diffuse in and out through the cavity wall. The reaction of materials prepared by template method is often in a limited size reaction space, which may have some limitations for other materials, but for PBNPs, this feature can control its size and shape. It is believed that more NPs will use its preparation technology in the near future. It can be seen that PBNPs prepared by template method can be accurately synthesized in an effective control region, and PBNPs with specific structures and properties can be prepared according to different applications of PBNPs. The structural improvement also further expands the application of PBNPs.

2.2.5 Preparation of PB by solvothermal method. The solvothermal method is an effective method developed in recent years to prepare nanomaterials with a certain special morphology.[61] The solvothermal method of PBNPs is to replace the solvent used in the hydrothermal method with other solvents of different polarities, or mix water and other solvents in different proportions.[54,62–64] The shape and size of PBNPs can be changed by affecting the growth of crystal nuclei or dispersing agents, reducing agents, and functionalized modifiers through solvents. Some of them are prepared without water, and the interstitial water does not participate in the formation of products. Thus, the sensing performance of PBNPs can also be improved. The initial solvent for PB preparation is only used for purification and etching. Purification is used in other methods, mainly hydrothermal methods, to dissolve and remove unreacted reactants. The main purpose of etching is to further change the morphology of the prepared PBNPs. Yu *et al.* used titanium(IV) and potassium hexacyanoferrate(II) trihydrate as solution A and solution B, respectively, to prepare Ti–PBA by co-precipitation method.[65] They then applied DMF as a solvent to prepare the Ti–PBA nanoboxes at 210 °C. In the study, the wall thickness of the nanobox can be controlled by the solvent heating time to form a uniform hollow structure, which will also be described in detail in subsequent chapters (Fig. 6A). It is expected to be used in efficient drug delivery systems with the continuous development of the solvent method and the continuous improvement of the growth mechanism of PB. Some solvents are not only

used in PB simple reaction solution, but also usually participates in the growth process in various ways to make a certain change in the structure of the product. We have used PVP as the reducing agent and 75% ethanol solvent as the reaction solution to prepare ultra-small PBNPs with a size of 3.4 nm.[66] The addition of ethanol first changed the molecular configuration of PVP, from chain-like to spherical. This transformation increased the steric hindrance between the crystal nuclei and reduced aggregation (Fig. 6B). The preparation method further verified the importance of solvent polarity to crystal size and uniformity. Compared with the conventional size, the magnetic properties of the small size PBNPs are also greatly improved (Fig. 6C). At the same time, it provides a new direction for the subsequent PB size control. After that, He *et al.* used the microwave-assisted reaction system as anhydrous ethanol to synthesize NaFeHCF nanoparticles through the monomer $Na_4Fe(CN)_6$ (Fig. 6D). However, the obtained product has poor dispersibility and large size, and the preparation process needs to be further optimized before it can be applied to biological materials.[64] Some examples include adding a dispersant to the reaction system and controlling the size by controlling the amount of monomers, reaction time and reaction temperature. The obtained nanoparticles are also not stereoregular like other conventional ways, which could be the result of the limited crystal growth due to the adsorption of the ethanol solvent on the individual crystal planes. However, from another point of view, regardless of the interference of PVP and external field, the mere presence of ethanol can also affect the growth of PB to a certain extent. Liu *et al.* selected 75% ethanol as the solvent, adjusted the pH value with Polyvinylpyrrolidone (PVP), ($Na_4Fe(CN)_6$) and sulfuric acid (H_2SO_4, 95.0–98.0%), and the reaction underwent directional self-assembly into shapes by solvothermal method to form regular PB nanoflowers.[67] In the reaction system, the hydroxyl group in the solvent ethanol plays a crucial role in the growth of PBNPs, and its hydroxyl group will adsorb with iron ions during the growth of

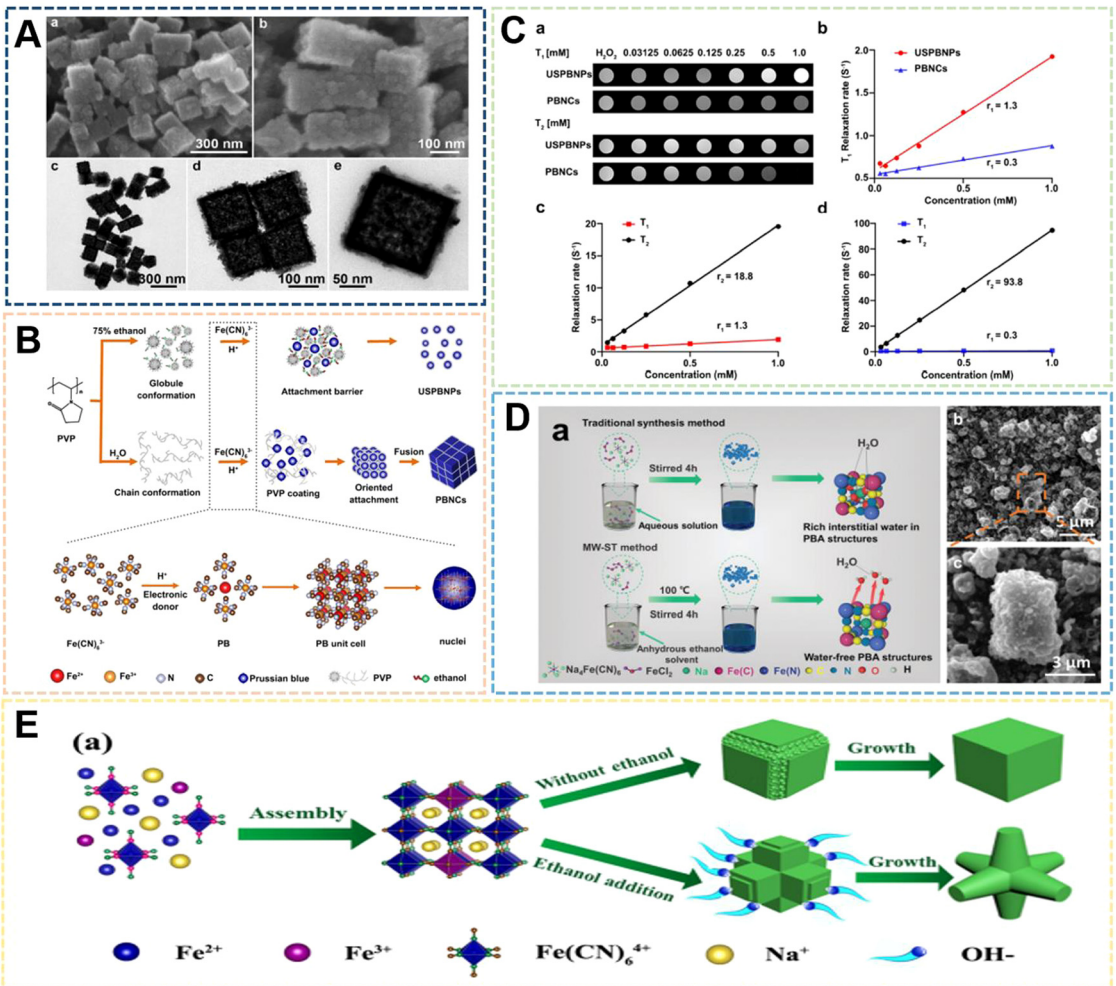

Fig. 6 (A) FESEM and (TEM) images of the TPB nanoboxes. Reprinted from ref. 65 with permission. Copyright 2020 Royal Society of Chemistry. (B) Proposed mechanism for growth of USPBNPs nanoparticles in ethanol/water. Reprinted from ref. 66 with permission. Copyright 2020 American Chemical Society. (C) T_1- and T_2-weighted MRI phantoms of USPBNPs. Reprinted from ref. 66 with permission. Copyright 2020 American Chemical Society. (D) Proposed mechanism for growth of PBNPs nanoparticles in ethanol. Reprinted from ref. 64 with permission. Copyright 2022 Royal Society of Chemistry. (E) Schematic illustration of growth mechanism for PB with different morphologies. Reprinted from ref. 67 with permission. Copyright 2020 American Chemical Society.

nanoparticles, which can prevent the growth of characteristic crystal planes (Fig. 6E). In the report, the DFT method was used to calculate the adsorption energies, and the energy value of C_2H_5OH adsorption on Fe attached to carbon atoms was the lowest among all configurations (−792.73 meV), which indicated that the –OH groups induced by C_2H_5OH were more inclined to the adsorption of Fe attached to carbon atoms, so the adsorption of –OH groups mainly occurred on the [100] crystal plane. During crystal growth, hydroxyl groups inhibit the growth of these sites by adsorbing iron attached to carbon atoms on the crystal edges, resulting in the PB material with a flower structure. The work further expounds the effect of ethanol as a solvent on the growth of PB, and also for the subsequent preparation of some special structures as biomaterials.

The preparation of PBNPs by the solvent method can affect the size and morphology of nanoparticles due to the characteristics of some solvents affecting crystallization, while the groups on the solvent molecules can also play a limiting or guiding role in the process of nucleation, growth and ripening. On the other hand, the addition of solvent can also make some compounds with low solubility in water participate in the synthesis of PBNPs. These compounds may bring some functional properties to PBNPs and enrich the application methods. According to some existing reports, the enzymatic activity and magnetic properties of PBNPs are optimized after the size reduction. The disadvantage of the solvent method is that when PBNPs are used as biological materials, the range of solvent types is small due to the consideration of biological safety. Therefore, the solvent method preparation process needs to be further improved to expand the types of solvents range to prepare different species and functionalized PBNPs.

2.2.6 Other synthetic methods. With the continuous update of several conventional and classical preparation methods of PBNPs, some new preparation methods are derived from traditional preparation methods.[68] These novel methods not only optimize the preparation process, but also often control the crystal growth through their methods to affect nanoparticles. The structure, size, and morphology of PBNPs can be optimized to improve the dispersion, stability, photothermal properties, and magnetic properties. Most of these novel preparation methods also use some characteristics of PBNPs to add an external field to the traditional preparation method, and the obtained products are often simple in process, or optimize the function, or change the morphologies to endow new properties. The simplest form of this external field is the external heating field. The electric oven is a good device to provide an external heat source. The use of electric furnaces to prepare PB is different from the pyrolysis of tube furnaces and muffle furnaces to prepare inorganic compounds. An electric oven can be controlled in a lower temperature range. Yamauchi *et al.* used an electric oven as an external field instead of hydrothermal heating to prepare PBNPs with PVP (K30) and $K_3[Fe(CN)_6]$ as monomers.[69] The obtained PBNPs can be divided into three sizes: small (about 20 nm), medium-sized (about 100 nm) and large (over 200 nm) (Fig. 7A).

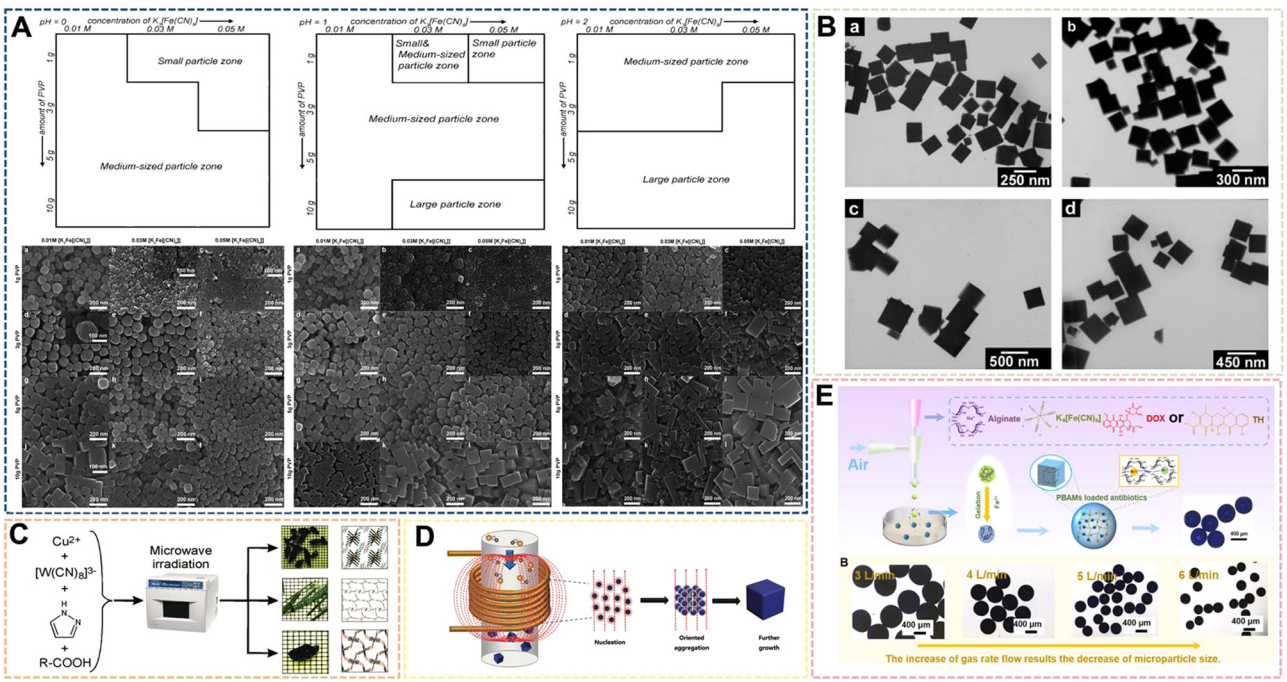

Fig. 7 (A) Particle-type classification of the PB products prepared when the pH value of solutions was fixed at 0, 1, 2. Reprinted from ref. 69 with permission. Copyright 2012 Royal Society of Chemistry. (B) TEM images of PB nanocubes prepared at 40 °C by sonochemical synthesis. Reprinted from ref. 70 with permission. Copyright 2006 American Chemical Society. (C) Schematic of the fabrication of PBNPs assisted by microwave-mediated self-assembly. Reprinted from ref. 71 with permission. Copyright 2011 American Chemical Society. (D) Schematic illustration of the fabrication of PBNPs assisted by an alternating-current magnetic field. Reprinted from ref. 72 with permission. Copyright 2019 Royal Society of Chemistry. (E) Illustration of PBAMs fabricated by gas-shearing strategy. Reprinted from ref. 73 with permission. Copyright 2022 Elsevier.

In recent years, the sonochemical method has also been applied to the preparation of PBNPs. The main mechanism of the sonochemical method is that the sound waves propagating in the liquid under the external ultrasonic field act on the reaction liquid to form bubbles, which in turn affects the nucleation rate, crystallization rate and crystallization rate growth size. He *et al.* dissociated $Fe_4[Fe(CN)_6]_3$ in acidic solution under ultrasonic conditions to prepare PBNPs of different sizes, the size of which depends on the reaction temperature under ultrasonic conditions, $Fe_4[Fe(CN)_6]_3$ concentration and the frequency of the applied ultrasonic field.[70] In the system, with the increase of reaction temperature or the increase of $Fe_4[Fe(CN)_6]_3$ concentration within a certain range, the size of nanoparticles will increase to a certain extent (Fig. 7B). However, there are still some problems to address: the product size distribution is wider, the preparation process needs to be further optimized, and the effect of ultrasonic frequency has not been effectively explained. Microwave-assisted heating has recently become a way of inorganic synthesis. Under the action of microwaves, crystals can grow rapidly in a short period of time. Compared with conventional synthesis methods, the compounds prepared by microwave methods have high crystallinity, small particle size and high physical adsorption rate. Energy efficiency is the main advantage of microwave heating because it is generated directly in the entire reaction system, rather than by conduction through the outer surface. Microwave heating is almost instantaneous and occurs without heating the air or container. Using the microwave method, Sieklucka *et al.* successfully prepared three novel cyano-bridged CPs (PBAs) with 1D, 2D and 3D morphologies.[71] After mixing, $[WV\text{-}(CN)_8]^{3-}$ and CuII were exposed to microwave radiation in the presence of Hpyr, and three novel CuII-$[WV(CN)_8]^{3-}$ inorganic–organic hybrid coordination polymers with cyanide-bridged compounds were formed (Fig. 7C). The magneto-endothermal method is a newly pioneered synthetic method that was developed in recent years. In the previous work, it was mainly used in the preparation of magnetic nanoparticles. Therefore, due to the magnetic properties of PB, its synthesis method has been greatly expanded along with the introduction of the magneto-induced internal heat preparation method. Magnetically induced internal heat is based on the magnetic properties of potassium ferricyanide and PBNPs. Under the action of an external magnetic field from the beginning of the reaction to the end of the reaction, the reactants and the products themselves generate heat to provide energy for the system. Our group was the first to propose a magneto-induced internal heat preparation method.[72] The PBNPs prepared at different current intensities had better dispersion, uniformity and crystallinity than the nanoparticles obtained by the conventional exogenous heating method (Fig. 7D). This method makes full use of the magnetic properties of PBNPs, but the disadvantage is that the PBNPs prepared by the method does not significantly improve the performance of catalysis and imaging, and the preparation technology needs to be further improved. It should be the focus of follow-up attention by other researchers. At present, there are few reports on the preparation of PBNPs by the magnetic internal heating method, and we only combine it with the hydrothermal method. Regarding the scope of application of medical materials, Huang *et al.* designed a gas shearing approach to prepare PB alginate microparticles (PBAMPs) using alginate as a substrate, which can achieve synergistic effects of PTT, antitumor and antibacterial properties.[73] The formed microparticles have good macropore-porosity due to the presence of alginate, and can be better used for drug loading. In the preparation method, the size of the PBAMPs can be controlled by adjusting the air flow rate. At present, the smallest uniform size is 300 nm, and the preparation of extremely small PBNPs by the method needs further development (Fig. 7E). However, the successful introduction of sodium alginate into this system proved that other polymer compounds with suitable viscosity can further participate in the preparation of PBNPs, and also enrich the modifiability and multifunctionality of PBNPs. Overall, the above novel methods and other reported methods are often optimized or modified from several traditional methods. Such manipulations not only make traditional methods more efficient, concise, and inexpensive, but also produce more reliable functionalized PBNPs.

3. Synthesis of Prussian blue analogues

In recent years, PB with a single original structure has been unable to meet the needs of its applications in many fields.[74–77] Therefore, a series of PB were designed and synthesized according to the different requirements of different application directions for the properties of materials. These nanoparticles are collectively referred to as PBA. At present, there are two methods of internal ion replacement and skeleton element replacement. These distinctions are also classified according to the location of structural changes and the resulting changes in characteristics. With the introduction of elements, some characteristics of different PBA will also be improved, so the composition and structure can also be designed according to actual application requirements. The following will mainly introduce the recent research on PBA as a biological material.

3.1 Replacement of elements in the framework of PBA

This type of compound includes those in which the iron element in the PB framework can be replaced by other transition metal elements. Its molecular formula can be written as $M_3[N(CN)_6]_2$ or $C_mM_x[N(CN)_6]_y{\cdot}xH_2O$, where M and N are the same or different transition metals, and the alkali metal ion C may also be absent. The usually selected metals to replace Fe elements are: Mn, Co, Ni, Cu, Zn and so on.[78–81] Bimetallic PBA includes complexes where part of the Fe element in the framework is replaced or the Fe element is replaced by two other metals. Some representative ones are Ni–PBA, Co–PBA, and Mn–PBA, and there are many more.[82–84] PBA with a changed structure not only retains some of the original characteristics of PB, but also strengthens some of the original characteristics or adds some new characteristics according to the requirements. The most representative PBA is the typical $Co_3[Co(CN)_6]_2{\cdot}xH_2O$ with a structure prepared from hexacyanocobaltate. Liao *et al.* chose a dual-precursor strategy to prepare Co–PBA of around

200 nm by co-precipitation method by mixing a mixture of cobalt nitrate and sodium citrate with potassium hexacyanoferrate(III) solution for synergistic PTT/PDT/chemical dynamic therapy.[85] In addition to photothermal properties, Co–PBA demonstrated chemokinetic therapeutic capabilities in the study. Its potential pathway is related to ferroptosis, and some results suggest its great potential as a contrast agent for MRI and PA (Fig. 8A). After further exploration, it was found that the underlying mechanism by which Co–PBA inhibits cancer invasion is the regulation of EMT protein expression. The magnetic resonance imaging ability of PB is mainly due to the Fe^{2+} and Fe^{3+} in its structure. If the magnetic properties are changed, in addition to changing its size by the preparation method, some other elements can be introduced to enhance the contrast agent effect. As the biological properties of rare earth elements are gradually being explored, more and more rare earth elements are introduced into the framework of PBNPs to enhance the nanoparticles in terms of their magnetic properties, fluorescence properties, photothermal and photodynamic properties. Wang *et al.* introduced paramagnetic Yb^{3+}, Gd^{3+}, and Tm^{3+} to replace part of Fe^{3+} in the PBNPs framework by hydrothermal method to enhance the photothermal and catalytic performance, and used FOI/MRI dual-mode imaging for adjuvant therapy.[86] The results show that the intravital imaging signal of PAI, CT and PTI increased significantly over time over a certain time frame after injection (Fig. 8B).

Inorganic nano-antibacterial agents can effectively prevent bacterial infection of the human body, and can be widely used in daily life and some postoperative patients, so it has great research significance. PB with a simple structure can use its photothermal properties and iron ion release to carry out a certain antibacterial effect, but its effect is general. Therefore, it is necessary to introduce specific elements into the framework to enhance the antibacterial effect. Since the advent of nano-silver, its highly efficient antibacterial effect has been used in many applications because of its super sterilization and disinfection effect, good antibacterial properties, biocompatibility and other advantages, and the smaller the size of nano-silver. Patra *et al.* selected $AgNO_3$, $K_3Fe(CN)_6$ and PVP to control the ratio of $AgNO_3$ and $K_3Fe(CN)_6$ by co-precipitation method to

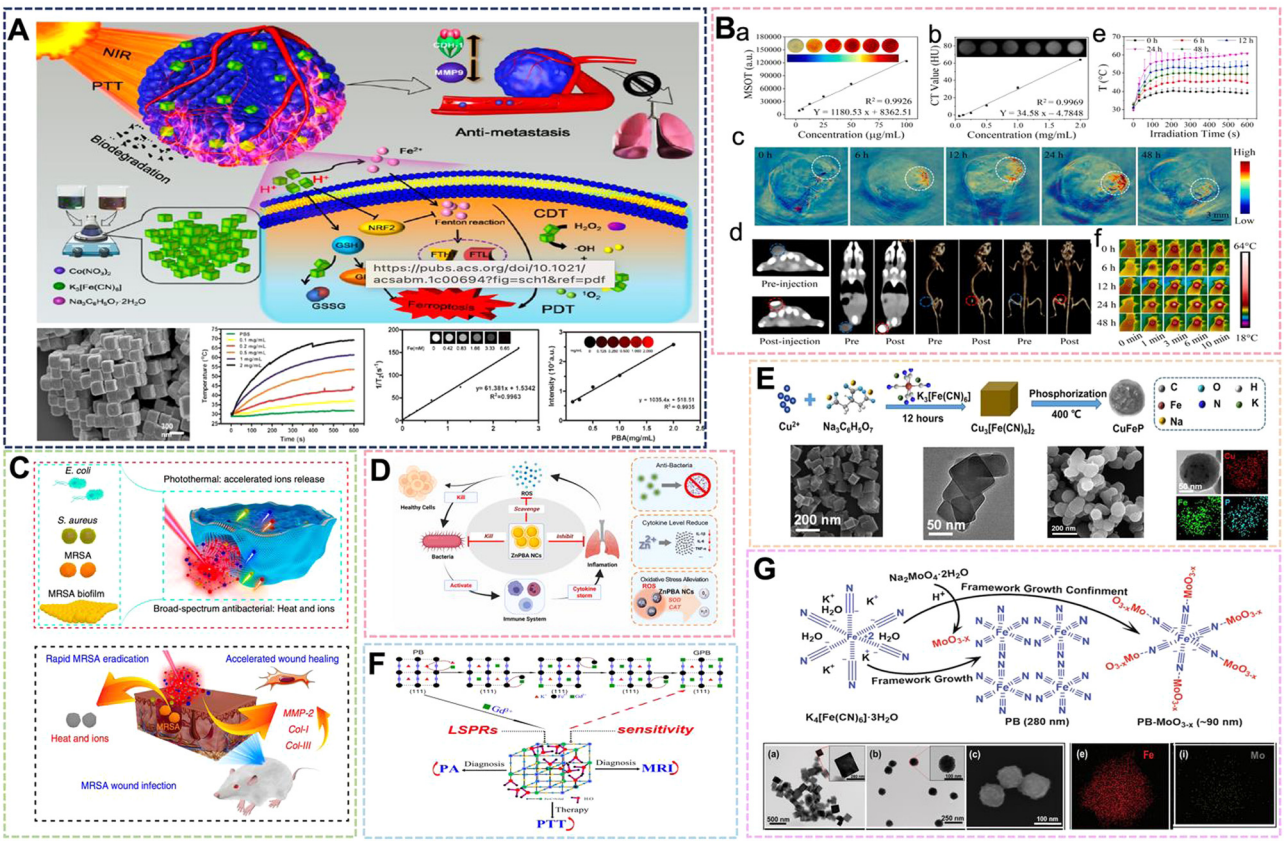

Fig. 8 (A) Detailed facile protocol to prepare biodegradable PBA nanoparticles and PTT/PDT/CDT therapeutic effect. Reprinted from ref. 85 with permission. Copyright 2021 American Chemical Society. (B) *In vivo* and *in vitro* PAI, CT and PTI of the PBA nanoparticles. Reprinted from ref. 86 with permission. Copyright 2022 Elsevier. (C) Antimicrobial mechanism of optimized heat and ion release synergistic effect of PBA nanoparticles. Reprinted from ref. 88 with permission. Copyright 2019 Nature. (D) Schematic mechanistic illustration of the therapeutics of Zn–PBA NCs against acute bacterial pneumonia. Reprinted from ref. 89 with permission. Copyright 2022 Elsevier. (E) Chematic illustration of the synthetic procedure of Cu–PBA. Reprinted from ref. 90 with permission. Copyright 2021 Elsevier. (F) Schematic of Gd^{3+} simultaneously optimizing the properties of Gd–PBA. Reprinted from ref. 92 with permission. Copyright 2016 American Chemical Society. (G) Schematic illustration of the growth of oxygen-deficient MoO_3-x NPs within the framework of Mo–PBA. Reprinted from ref. 93 with permission. Copyright 2019 Royal Society of Chemistry.

prepare Ag–PBA with a size of 50–60 nm, which is expected to be used in drug delivery, nanomedicine and antibacterial applications.[87] At the same time, as one of the essential trace elements for the human body, zinc plays an extremely important role in important physiological processes, such as human growth and development, reproductive inheritance, immunity, and endocrine. Therefore, PBA doped with zinc will play a role as a medical material. Wu *et al.* mixed the PVP solution of $K_3[Fe(CN)_6]$ and the PVP solution of $ZnCl_2$ with HCl to adjust the pH value, and obtained Zn–PB nanocubes by hydrothermal method at 80 °C for 20 h.[88] Both Zn and Fe are transition metals with similar atomic numbers, and Zn has more valence electrons than Fe. In this move, doping Zn to replace Fe^{2+} in the PBNPs framework improves the photothermal and ion-releasing synergistic antibacterial effect of Zn–PBA (Fig. 8C). The geometric and electronic structures of Zn–PBA with different doping levels were modeled through theoretical calculations, and the effect was improved. This is due to the band gap narrowing effect and the increase of Zn doping density. The preparation method firstly configures the solution of two metal salts, which is synthesized after mixing. This is also an outstanding embodiment of the preparation strategy of PBNPs dual precursors in the preparation method of PBA. Subsequently, Shi *et al.* prepared Zn–PBA nanocatalysts from $ZnCl_2$, $K_3[Fe(CN)_6]$ by self-assembly method. It was demonstrated that Zn–PBA can effectively scavenge superoxide anion radicals, hydrogen peroxide and hydroxyl radicals with excellent SOD and CAT mimetic activities.[89] Through the comprehensive treatment of antibacterial and antioxidant properties of acute bacterial pneumonia, it also showed broad-spectrum antibacterial ability against *Escherichia coli*, *Staphylococcus aureus* and other bacteria (Fig. 8D). Under the research studies, the clinical application progress of Zn–PBA as a nanozyme and the research speed of PBA design were further advanced. It has been mentioned above that the nanoenzyme activity of PBA is used to inhibit inflammation, so it is crucial to introduce necessary elements to enhance the catalytic performance. In their paper, Li *et al.* selected $Cu(NO_3)_2{\cdot}3H_2O$, $K_3[Fe(CN)_6]$ (0.4 mmol) and $Na_3C_6H_5O_7{\cdot}2H_2O$ to prepare 100 nm Cu–PBA, and then the product was phosphated to convert the cubic Cu–PBA into spherical CuFeP (Fig. 8E). The introduction of $Cu^{+/2+}$ into the material structure utilizes its Fenton-like reaction to enhance the enzymatic activity of PBA, while exhibiting a photothermal conversion rate of 66.9% and a tumor growth inhibition rate of 83.7%.[90] The dual catalytic center or multiple catalytic active centers also need more in-depth research in the design of nanoenzyme materials. Yamauchi *et al.* designed a nanocatalyst prepared by thermal conversion through cyano-bridged coordination polymers, and the crystal orientation growth was managed by controlling the concentration of trisodium citrate dihydrate (TSCD). In the system, Mn–citric acid complexes tend to release Mn^{2+} ions stably and slowly. The interaction between Mn–Ru oxides is further developed to form several types of cyano-bridged coordination polymers (abbreviated as MnCNMn, MnCNCo, or MnCNRu, respectively), in which Mn–Ru oxide catalysts can selectively reduce the two-electron pathway.[91] Its excellent H_2O_2 generation performance is also expected to play a role in tumor treatment, and it is expected to become a new type of nano-enzyme material.

The role of PB in diagnosis and treatment is often discussed, and another one of its properties as a biological material is photothermal therapy. Some PBAs have already been introduced to utilize their photothermal properties for antibacterial applications. With increasing research studies, some PBAs with excellent photothermal properties have been gradually designed and developed. Through controlling the Gd^{3+} sites in the framework structure of PBNPs, Shi *et al.* prepared Gd–PBs with tunable LSPR to improve the imaging efficiency of PTT and PA for lower dose and laser flux tumors.[92] By introducing elemental Gd and adjusting its site, the work overcame the deficiency wherein the maximum near-infrared absorption peak of PBNPs in the range of 690–720 nm cannot be optimized near the laser wavelength. This enabled the enhancement of the photothermal conversion rate and further expanded the application of PBA in the field of biomedical materials (Fig. 8F). Recently, Xu *et al.* selected $K_4[Fe(CN)_6]$ and Na_2MoO_4 with PVP as a reducing agent and dispersant to prepare Mo–PBA with a size of about 90 nm by hydrothermal method for PTT/PDT synergistic therapy.[93] MoO_3-x modified Mo–PBA has strong absorption in the near-infrared range, and the molar ratio of Na_2MoO_4 in the reaction system was increased from 0 to 0.5. It was found that the absorption intensity of PB-MoO_3-x NCs in the Vis-NIR region increased significantly (Fig. 8G). To examine the photothermal properties of Mo–PBA, under 808 nm laser (1.0 W cm^{-2}, 10 min). The temperature of the PB-MoO_3-x NCs rose from 23 °C to 63 °C, while that of PB alone increased from 23 °C to 38 °C, that is showing high photothermal conversion efficiency. The enhancement of these properties is attributed to the strong near-infrared absorption of MoO_3-x and the oxygen vacancy-induced surface plasmon resonance effect. The study expands the application of polyacid compounds in the preparation of PBA, and also increases the options for introducing elements for subsequent preparation. The most important thing is that the introduction of MoO_3-x in this way is different from conventional PBA. It is not just a simple element replacement, but an extension of the skeleton. Preparing PBA in this way will also become a new strategy for PBA in the future.

According to the reported research, the PBA materials formed by other transition metal ions replacing Fe ions in the PB structure have gradually shifted from the research fields of ion battery electrodes and photoelectrochemical water splitting to the biomedical field.[94] The replacement of Fe element in the PB framework may change the basic properties to a certain extent, such as the enhancement of the electron–hole effect, contrast effect or the enhancement of photothermal properties or magnetocaloric properties brought by certain elements. Strengthening will provide strong support for the application of PBA to biological materials. With the continuous optimization of the preparation technology of PBA replaced by skeleton elements, the size of some PBA is reduced. Thus, it is expected to further develop and expand the application of PBA in the fields of diagnosis and treatment, imaging, drug release and other biomedical fields.

3.2 PBA with altered interstitial ions

The interstitial ion K^+ in the conventional PB can also be designed to be replaced by Na^+, Rb^+, Cs^+ plasma.[95] The capacity (mA h g^{-1}), redox potential (V) and capacity fade rate (%/cycle) of the PBA material were all affected by intercalating different cations to replace interstitial ions. The current properties of these materials are prominent in electrochemistry. So, in the current research, this type of PBA is mainly used in the field of biosensors.[96] For example, Chen *et al.* used $Na_4Fe(CN)_6{\cdot}10H_2O$ and PVP to prepare Na/PBA by co-precipitation method and chemical etching two-step method. Chemical etching increased the specific surface area of Na/PBA, and the material had excellent electrochemical properties. The fly in the ointment is that the size of the PBA in the work is not only not excellent in uniformity, but its size is between 1 μm and 2 μm. Such a large size also limits its application in the biomedical field, resulting in it only expected to be used in biosensor devices. Similarly, by changing the reducing agent, the porosity of the structure can be enhanced, so that the interstitial ions can enter the structure more efficiently.[97] Tan *et al.* added a large amount of ascorbic acid and iron ions during the preparation of PBNPs to produce chelation. This limited the growth and maturation process to a certain extent, and then thermally vacuum-dried the product at 200 °C, resulting in the formation of PBNPs with enhanced porosity. Sodium ions could then penetrate deeper into the PB crystals compared to conventional preparation methods. In the context of biosensors attracting much attention, how to effectively improve their electrochemical properties is crucial due to the versatility of PBNPs.[98] Therefore, He *et al.* developed a microwave-assisted solvothermal (MW-ST) method to synthesize high-quality Na/PBA.[64] In the paper, anhydrous ethanol was used as the reaction solvent to prepare high-quality NaFeHCF nanoparticles. Interstitial water does not participate in the formation of NaFeHCF products during the reaction. Meanwhile, less interstitial water helps the material maintain its structural stability during Na^+ insertion/extraction and reduces the occurrence of side reactions. The assistance of the microwave method providing external energy to the reaction is accelerated at slightly elevated temperature. The data show that the samples synthesized at 100 °C for 4 h exhibit good rate performance, cycle life over 500 cycles, and high discharge specific capacity of 150 mA h g^{-1}. The novel microwave-assisted solvothermal (MW-ST) method for non-aqueous synthesis used in the study confirms that the anhydrous technique can synthesize NaFeHCF with excellent electrochemical properties, but its morphology, especially the size, has not been regulated in the preparation process. If the problem is solved, its products may be further expanded in other properties. From the existing reported data, it can be concluded that when the interstitial ions change, the electronic environment of the Fe^{2+}/Fe^{3+} redox center in the PBA structure will be significantly affected, thereby enhancing the electrochemical properties of the PBA. However, this part of the research only discusses the basic electrochemical properties of PBA and its application as an electrode material. At present, there are few reports on the replacement of interstitial particles in PB for biological applications. After the void ions in the PBNPs structure are replaced, the excellent electrochemical properties and controllable structure of this type of PBA can be used in biosensors and other biomedical fields for further development. In addition to potential applications as materials such as biosensors, when interstitial ions are replaced by some therapeutic cations, they may have therapeutic effects on some diseases when they enter designated sites. This part of the idea is also expected to be verified by many researchers working together.

4. PB(PBA)-based hollow structures

With the deepening of research on PBNPs, it has been further discovered that PBNPs with specific nanostructures can exhibit unique properties or enhanced performance. Due to the special structural properties of PB, the hollow structure offers fascinating physicochemical properties and extensive applications without changing the original elemental composition. HMPBs have a better surface area and show excellent performance in catalysis, drug carrier, active factor loading, and electrochemical storage. Therefore, HMPBs have great application prospects in the fields of nanozymes, controlled release, and biosensors.[99–101]

A large number of HMPBs have been prepared according to numerous preparation methods and applied in the biomedical field. Among the numerous structures, HMPBs are mainly divided into ''closed structure'', ''open structure'' and some composite structures. At present, the main methods for preparing HMPBs are also divided into ''soft template method'' and ''hard template method''.[102] The ''soft template method'' usually uses micelles, microspheres and microemulsions as the core to control the surface of the reaction system. HMPBs can be formed by simple water washing or demulsification after the reaction. The method can form closed PB nanoshells when the reaction time, temperature and monomer amount are sufficient. The soft template method is easy to construct in the preparation system and does not require complicated equipment. However, its size control and the preparation of PBNPs with special shapes are relatively difficult, which also becomes the disadvantage of this method. The ''hard template method'' involves the preparation of HMPBs with other rigid inorganic compounds as the core. Usually, some strong acids are selected for etching to obtain HMPBs.[65,103–106] The HMPBs obtained in this way are partially closed structures. The nanoparticles of the core are irregular, restricting the growth in a certain orientation, or the thickness of the outer wall is too small and partially etched during the etching process to form a certain amount of open area. The two structures also have their own advantages in some applications. For example, in controlled release, the closed structure is suitable for some small molecule drugs to be released by the porosity of PBNPs. On the other hand, the open structure can load some active factors with larger molecular weight, such as some bone growth peptides for the treatment of osteoporosis and related diseases. Chen *et al.* achieved triple synergistic therapy utilizing the higher BET surface area and larger average pore size of HMPBNPs.[107] First, HMPBNPs with a size of 100 nm were prepared by hydrothermal method and hydrothermal etching. Then, HMPBNPs encapsulated Cur and

stabilizer Pluronics F127, and then 5-Fu were loaded into the structure by physical adsorption and ferric amine coordination. The endogenous H_2S reacts with PB during drug release near the tumor, and converts it into PW with higher ferrous (Fe^{2+}) content for synergistic treatment of colorectal cancer with Cur and 5-Fu (Fig. 9A). In addition, while the hollow structure enhances the loading rate, the accelerated release of the loaded molecules can be carried out through the photothermal properties. Lian *et al.* prepared HMPB by hydrothermal method and hydrochloric acid etching.[108] In the etching step, the hydrothermal method was used to adjust the pH value, and HCl was used as the etchant. Zinc ions were doped into the framework of HMPB by ion exchange. Then, Zn-HMPBA can promote the release of loaded lonidamine (LND) and the dissociation of zinc ions through the photothermal effect, thereby achieving the effect of down-regulating the level of glycolysis (Fig. 9B). As mentioned above, the photothermal properties are used to control drug release, so when used as a drug carrier, the high loading rate of HMPBA can also be used for PTT at the same time. Thus, we designed and prepared a zwitterionic polymer-modified HMPBs-targeted drug-loading system (HMPBA(DNR + AraC)@PEI-ZS-E5) for the combined chemotherapy-photothermal therapy of AML.[109] In the material preparation, a conventional hydrothermal method was used to prepare 100 nm PBNPs with $K_3[Fe(CN)_6]$ and PVP, and then HMPBs were formed by etching with HCl. Subsequently, PEI, ZS (copolymerization of AA and DMAPS), and E5 were externally connected. The experimental results show that the material exhibits outstanding photothermal conversion performance, photothermal stability, protein adsorption resistance, and biocompatibility (Fig. 9C). Meanwhile, HMPBs(DNR + AraC)@PEI-ZS-E5 has higher drug loading capacity compared with conventional PBNPs. Liu *et al.* also prepared HMPBNPs from $K_3[Fe(CN)_6]$ and PVP by a simple hydrothermal method.[110] The application of red blood cell (RBC) membrane-coated HMPB (HMPB@RBC) NPs loaded with dox for chemo-photothermal synergistic therapy was also first reported. The modification of the RBC membrane endowed the HMPB NPs with biomimetic properties, which significantly enhanced the immune evasion ability of Dox/HMPB@RBCNPs and increased their retention time in blood circulation (Fig. 9D). To further demonstrate the multiple application properties of PBNPs as drug carriers, Xue *et al.* developed a multifunctional nanotherapeutic by loading indocyanine green (ICG) and dox onto the surface or cavity of HMPBNPs.[111] An agent termed ICG/Dox/HMPB@PEI was investigated as a phototherapeutic agent for *in vivo* fluorescence imaging and triple-combination therapy of light-induced chemotherapy, photothermal therapy (PTT), and photodynamic therapy (PDT) (Fig. 9E). In addition, the drug carrier can respond

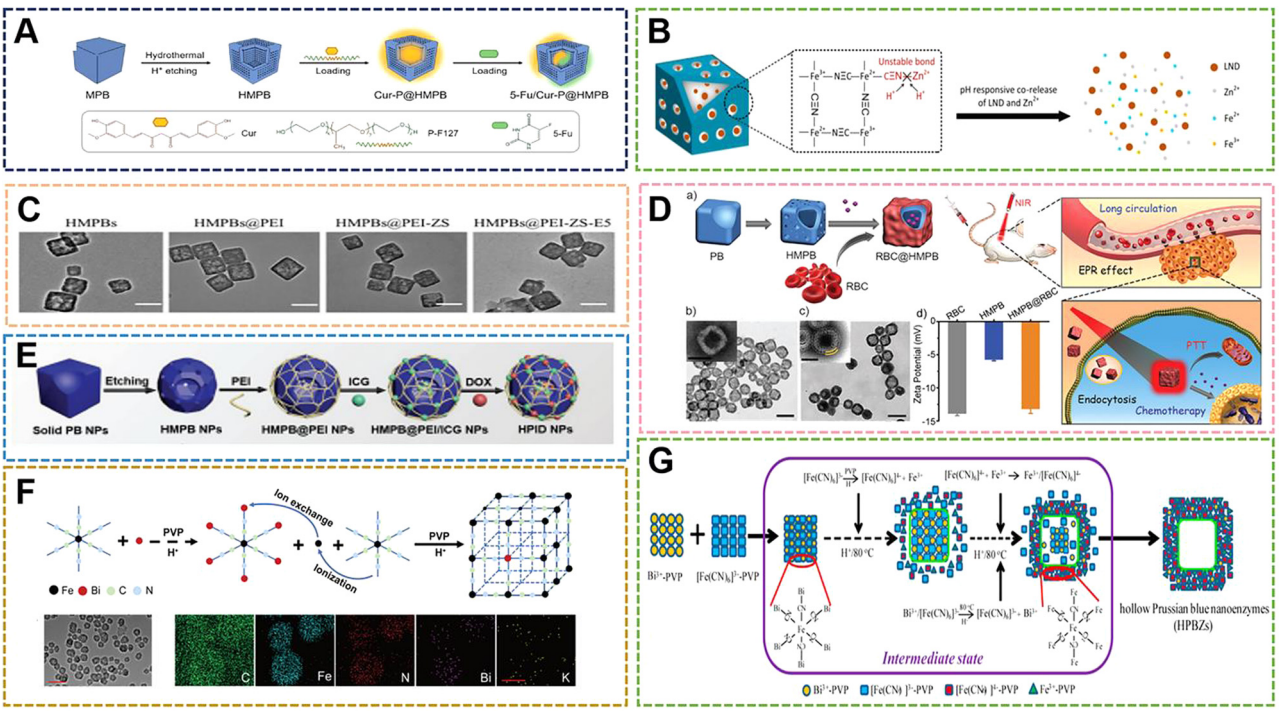

Fig. 9 (A) Schematic Illustration of Cur-P@HMPB NPs and 5-Fu/Cur-P@HMPB NPs Preparation. Reprinted from ref. 107 with permission. Copyright 2022 American Chemical Society. (B) The construction process of LND@HMPB-Zn nanosystem and its biological mechanisms of synergistic effects of dual glycolysis regulation and photothermal therapy in inhibiting the metastasis of melanoma to the lungs. Reprinted from ref. 108 with permission. Copyright 2022 Elsevier. (C) TEM images of HMPB. Reprinted from ref. 109 with permission. Copyright 2021 Royal Society of Chemistry. (D) Illustration of the preparation of drug loaded HMPB@RBC NPs, and the synergistic photothermal-/chemotherapy of cancer. Reprinted from ref. 110 with permission. Copyright 2017 Elsevier. (E) Schematic of the synthetic procedures of HPID NPs for NIR laser-activated tri-modal combination therapy of cancer. Reprinted from ref. 111 with permission. Copyright 2019 Royal Society of Chemistry. (F) Diagram of HPBZ possible formation mechanism. Reprinted from ref. 113 with permission. Copyright 2022 Wiley. (G) Schematic diagram of HPBZ formation. Reprinted from ref. 115 with permission. Copyright 2019 American Chemical Society.

to tumor-specific acidic microenvironment and local thermal shock, resulting in controlled release of loaded dox. Although HMPBNPs have been studied as drug carriers, the structure selected for their application still has certain shortcomings, such as the openness of the pores, which leads to the loss of drugs in the blood circulation and to a certain extent the immune response. In the process of drug delivery, the imaging properties, photothermal properties, and enzymatic activities of HMPBNPs should be fully utilized to construct an integrated diagnosis and treatment system, and implement multiple synergistic treatment programs. For synergistic treatments, such as chemical-photothermal and chemical-photodynamic approaches, HMPBNPs have gradually developed new preparation technologies based on the initial preparation technology, and their application mechanism *in vivo* is also being further explored and improved.

HMPBNPs as biomaterials still retain ROS scavenging ability in addition to being excellent drug carriers. Wang *et al.* synthesized PBNPs with $K_3[Fe(CN)_6]\cdot 3H_2O$ and PVP, and then etched them with HCl to form HMPBNPs, and utilized their POD activity to convert H_2O_2 to the more active $^{\bullet}OH$ species at low concentrations to inhibit bacteria.[112] In the system, HMPBNPs exhibited excellent peroxidase-like catalytic activity and could generate a large amount of $^{\bullet}OH$. However, all of this is in the form of solution, a fluid liquid that cannot act on the wound surface for a long time when it acts on the external surface wound. Due to the demand for antibacterial materials and the good antibacterial properties exhibited by PBNPs, polymer compounds were introduced to form coatings or gels for application to better treat the wound surface. With the continuous expansion of the application range of HMPBs, some HMPBAs have also been gradually designed and developed Cai *et al.* prepared Bi-HMPBAs by hydrothermal method with $Bi(NO_3)_3$ and $K_3[Fe(CN)_6]$, and used its nanoenzyme activity to regulate the microenvironment of osteoporosis (OP). They verified that the Bi-HMPBAs osteoclast formation and resorption can be inhibited by regulating oxidative stress, thereby effectively delaying the further development of OP.[16] High ROS levels, a characteristic pathological change in arthritis, increase hypoxia-inducible factor 1α (HIF 1α) levels and promote synovial inflammation. Fan *et al.* used bovine serum albumin (BSA) bubble template to prepare Mn-HMPBAs with $MnCl_2$ and $K_4Fe(CN)_6$ by co-precipitation method, which synergistically scavenged ROS and alleviated hypoxia to reduce inflammation.[113] It can be seen that both HMPBNPs and traditional PBNPs have certain regulatory and therapeutic effects on OP and OA (Fig. 9F). Lou *et al.* prepared $CdCl_2$, PVP, sodium citrate and $K_3[Co(CN)_6]$ into solution A and solution B, respectively, and prepared 1.4 μm Cd–PBA by coprecipitation method.[114] Afterwards, a two-step vulcanization strategy was established to fabricate novel CdS cage particles with thioacetamide, $NH_3\cdot H_2O$, and Na_2S. Since the Cd–PBA surface was protected by the introduction of PVP during the synthesis process in the first vulcanization reaction, the etching process started at the subsurface of the structure and the ions diffused outward. While the surface of the Cd–PBA cube inside the CdS cage is not protected in the second sulfidation reaction, the etching process will start from the surface. The structures of the Cd–PBA@CdS cage and CdS@CdS cage were obtained by two separate vulcanization reactions. In the study, the CdS@CdS cage exhibited enhanced photocatalytic hydrogen production activity under visible light irradiation compared to ordinary CdS cubes and CdS cages. Nevertheless, in the paper, only the data comparison of the CdS@CdS cage, CdS cube and CdS cage was carried out, and the intermediate product of the Cd–PBA@CdS cage was ignored. Due to the good photocatalytic activity of the CdS@CdS cage, according to the physicochemical properties of PB, we speculate that the Cd–PBA@CdS cage may have certain excellent properties on nanomedicines. Tian *et al.* selected Bi^{3+}-assisted synthesis of hollow PB nanozymes (HPBZs), which can not only efficiently reduce ROS levels, but also scavenge nitrogen species.[115] Its unique hollow structure endows HPMBA with a large specific surface area to counteract RONS, putting forward treatment options for disease-modifying ischemic stroke (Fig. 9G). An interesting point in the study is that the HPMBA were not obtained by conventional etching methods. A simple preparation method is bismuth nitrate, potassium ferricyanide, PVP, and hydrochloric acid (1 M) mixed under magnetic stirring, and then kept at 80 °C to construct HPMBA. When the bismuth concentration is increased to 0.5 mM, the size of HPMBA may be less than 100 nm. By optimizing the preparation technique, it was found that when the concentration of hydrochloric acid was increased to 2 M at 80 °C, no HMPBA was observed, suggesting that the cavities of HMPBA in this study may not be caused by acid etching. However, when Gd^{3+} ions of similar radius are selected instead, HMPBA is still not obtained under the condition of other conditions remaining unchanged. These results suggest that the formation of HPBZs is related to the intrinsic properties of Bi^{3+}. This is a very interesting finding, and will lead researchers to consider other ways to control the preparation of HMPBs aside from simple etching.

Overall, HMPBNPs retain most of the properties of PBNPs, including many of the imaging properties mentioned earlier. Chen *et al.* used hydrochloric acid to etch PB to form HMPB, which can continuously foam and vaporize the encapsulated liquid when irradiated by NIR, thereby enhancing the signal of ultrasound imaging.[116] At present, there are relatively few reports on HMPBNPs in the field of biomedicine, and their research has not yet formed a complete system, mainly because the preparation technology and structural control of HMPBNPs as biomaterials need to be further improved and perfected. Therefore, the innovation of HMPBNPs preparation technology is a key step, and its products have important development significance in many application fields.

5. PB(PBA) composites

5.1 PB(PBA)/organic materials

Hybrid nanostructures are a class of functional materials with a wide range of applications, and structural control has been shown to have multiple uses to optimize the functions and properties of nanomaterials.[117,118] Organic polymers play an important role in the synthesis of hybrid nanomaterials, so they

play a huge role in the preparation of PBNPs.[119–123] In terms of external modification, when materials such as PVP,[25] chitosan,[124] and citric acid[125] are used as reducing agents, dispersants and protective agents, they are often wrapped on the surface of PB to provide some modification points or give them better dispersibility and biological compatibility. Sometimes, some suitable polymers are selected to carry out certain bonding on the outside of PBNPs, and then the groups on the polymer tend to be endowed with more functional sites. Therefore, different external modifications will also lead to the generation of some PBNPs with different specific properties to a certain extent. With the emergence of more organic polymer-modified PBNPs, the application range has been further expanded.

Initially, some organic compounds were used as reducing agents to participate in the preparation of PB. PBNPs prepared in this way often adopt a single-precursor synthesis strategy, which has the advantages of a simple preparation process, simplified purification process, and less control variables. Ye *et al.* proposed a near-infrared (NIR) light-responsive CO delivery nanocarrier involving PEGylated iron carbonyl-derived PBNPs.[126] In their study, 100 nm PBNPs were prepared from hexacyanoiron(III) and polyvinylpyrrolidone. The pH was adjusted with HCl. PVP acted as a reducing agent and dispersing agent, and the size was simultaneously controlled with pH. Then, the PNNPs prepared at a certain concentration were stirred with 1% $Fe(CO)_5$ work solution for 24 h to form PB-CONPs, which endowed them with the ability to release CO. Finally, poly(ethylene glycol)bis (amine) was combined with PB-CONPs through chelation to impart targeting. The utilization of carbon monoxide (CO) in the system can induce mitochondrial dysfunction to induce apoptosis in cancer cells, thus becoming an emerging therapeutic approach in recent years. PBNPs can be used as drug carriers, and the near-infrared irradiation intensity and irradiation time can be used to adjust the CO treatment and CO/photothermal synergistic treatment, which can effectively inhibit tumor growth under the selected treatment plan (Fig. 10A). The synthetic method proposed in the study is expected to derive a number of metal carbonyl compounds, which then lead to a series of promising nanomaterials for biomedical applications. The reducing agents with the same effect as PVP are also commonly used in the preparation of PB, such as citric acid and ascorbic acid.

As more polymer compounds are added to the preparation process of PB, the external modification of some polymers can make some PBNPs prepared by traditional methods have better dispersion, stability and uniformity. The size and morphology of PB can also be restricted by the combination of its functional group and vacant Fe^{3+}. In order to solve the phenomenon of poor dispersibility of PB prepared with citric acid as a reducing agent, Shiba *et al.* added citric acid solution to the reaction system containing $Fe(NO_3)_3$, $K_3Fe(CN)_6$ and HNO_3, where acid was added to avoid crosslinking between the gelatin molecules. Coagulated by the $Fe(CN)_6^{3-}$ ions, gelatin-protected monodisperse PBNPs with an average size of 70 nm were prepared at 35 °C and pH 0.95.[127] In the system, citric acid acts as a reducing agent and also controls the size, while gelatin as a protective colloid improves the uniformity and dispersion. Coincidentally, in order to further optimize the properties (such as structure and size) prepared by citric acid as a reducing agent, Liu *et al.* chose polyethylene glycol (PEG) to modify the surface of PB nanocubes (PBNCs) to form a coating through layer-by-layer (LBL). The material still had high photothermal stability after modification, and *in vivo* T_1-weighted magnetic resonance (MR) and photoacoustic tomography (PAT) double-modal imaging were obtained. The effect demonstrates its application as a multifunctional nanoprobe for therapeutic diagnosis.[128] The functionalization of PEG improves the physiological stability of nanoparticles, and solves the poor dispersibility and instability of PB prepared by citric acid as a reducing agent in a physiological environment. The properties exhibited by the optimized PB–PEG further promote PB applications (Fig. 10B).

With the application of PB in the biological field and the development of peptide drugs, peptide compounds have attracted increasing attention in the preparation of PB due to the abundant and large number of groups that can coordinate with Fe^{3+} on the peptide. Zhu *et al.* developed a direct decomposition-assisted synthesis (DDAS) strategy for the efficient and scalable synthesis of polymer/inorganic hybrid nanoparticles with well-defined shapes and tiny sizes (20 nm).[129] Incorporation of ferricyanide into a polypeptide resulted in the disassembly of the large hexagonal packing structure of the polypeptide alpha-helix into small aggregates. Subsequent coordination polymerization of ferricyanate groups and Fe^{3+} in aqueous medium resulted in polypeptide@PB hybrid nanoparticles with a core–shell structure of about 18 nm (Fig. 10C). Compared with conventional PBNPs, the peptide@PB of DDAS exhibits excellent electrochemical activity, which can be applied in biosensing and nanodevices. The fly in the ointment is that the homogeneity of PBNPs prepared in this way is poor. If the homogeneity can be further improved and the preparation of small size can be ensured, it is also expected to be further applied as a diagnostic agent. PBNPs prepared by co-precipitation method is often an insoluble product if no dispersant is added during the preparation process. This insolubility and poor dispersibility greatly limit the application of PB prepared by this method. However, Zha *et al.* modified the surface of insoluble PBNPs with oleylamine (OA) and lipid–polyethylene glycol (DSPE–PEG) by a two-step method (LBL) for loading and delivering dox for chemo-photothermal synergistic therapy.[130] When the mass ratio of dox to DSPE–PEG 2000 lipid was 1 : 10, the drug loading efficiency and content were calculated to be 98.0% and 9.2%, respectively. At pH 4.0, the loaded dox was released within 48 h, and its pH-responsive release properties are mainly attributed to the presence of amine groups in dox and DSPE–PEG lipids, which can be protonated at slightly acidic pH, rendering the drug and drug carrier hydrophilic and leading to faster release. Meanwhile, the heat generated by NIR laser irradiation can not only change the lipid chain structure of PEGylated PB-Dox NPs, but the photothermal effect can also promote the cellular uptake of PEGylated PB/Dox NPs (Fig. 10D). Some organic compounds as surfactants, can modify PBNPs externally, and use the kinetics and thermodynamics during the preparation process to influence the structure and crystal phase. The previous work by Huang *et al.*

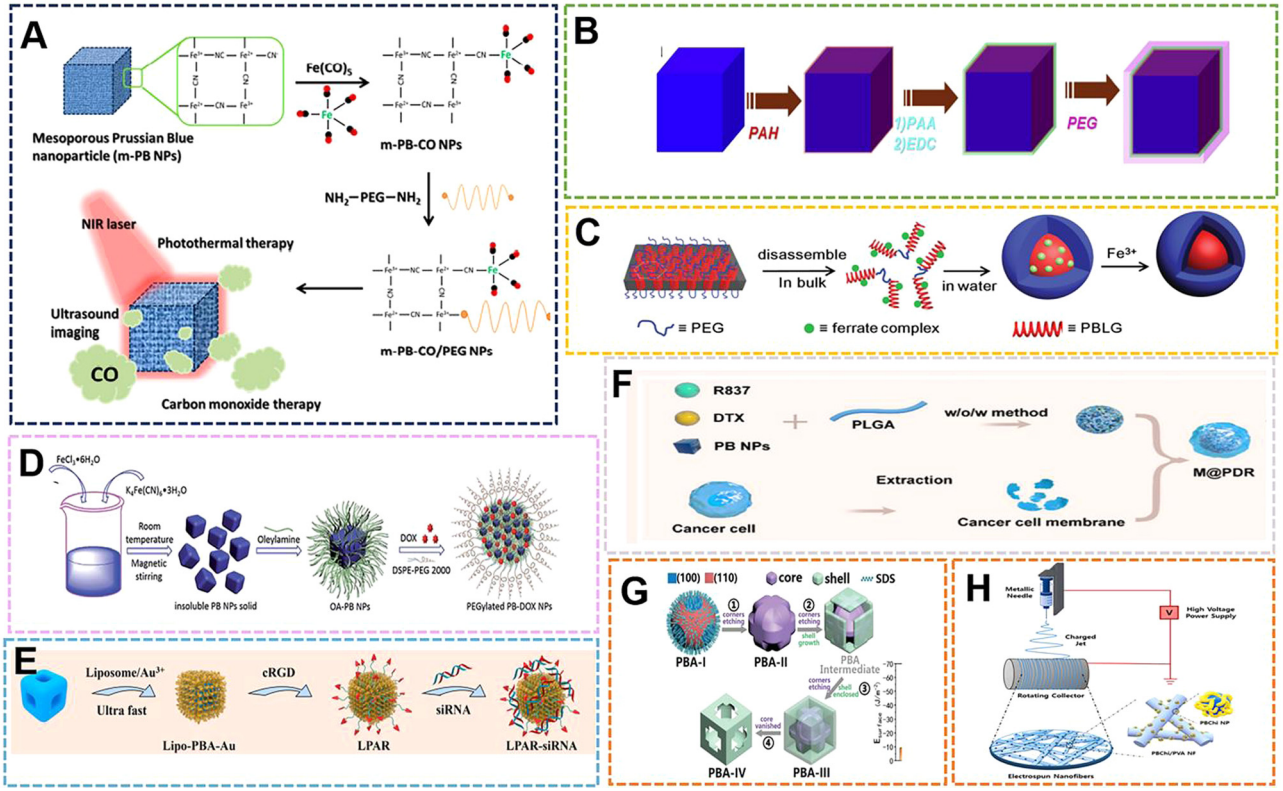

Fig. 10 (A) The m-PB-CO/PEG NPs can be triggered by NIR laser to initiate CO and photothermal therapy and US imaging applications. Reprinted from ref. 126 with permission. Copyright 2016 American Chemical Society. (B) MR contrasting ability of PB-PEG NCs. Reprinted from ref. 128 with permission. Copyright 2014 Elsevier. (C) Schematic illustration of direct disassembly-assisted synthesis of tiny polymer nanoparticles. Reprinted from ref. 129 with permission. Copyright 2015 Royal Society of Chemistry. (D) Schematic illustration of preparation of PEGylated PBNPs. Reprinted from ref. 130 with permission. Copyright 2015 Royal Society of Chemistry. (E) Schematic illustration of the construction of the targeted theranostic device (LPAR-siRNA). Reprinted from ref. 86 with permission. Copyright 2022 Elsevier. (F) Schematic illustration of M@P-PDR. Reprinted from ref. 132 with permission. Copyright 2021 BioMed Central Ltd. (G) Schematic illustration of the nanostructural evolution from PBA-I to PBA-IV. Reprinted from ref. 131 with permission. Copyright 2020 Wiley. (H) Preparation of electrospun PBChi/PVA NFs with ROS scavenging and wound healing properties. Reprinted from ref. 135 with permission. Copyright 2022 Elsevier.

involved the preparation of morphology-specific Mn–Co–PBANPs with $K_3[Co(CN)_6]$, $(Mn(CH_3COO)_2{\cdot}4H_2O)$ and $(CH_3(CH_2)_{11}OSO_3Na$(SDS)). The work prepared four morphologies of Mn–Co–PBANPs as follows: chamfered cubes, prominent crosses on the outer surface, crosses inside the SDS shell, and open cross hollow structures with increasing reaction time, respectively. This is mainly due to the high surface energy of the (111) plane.[131] Due to the surface energy of the (100) surface, the anionic SDS is more inclined to adsorb on the (111) surface, resulting in a higher growth rate of the (111) surface (Fig. 10G). The reaction process of the Mn–Co–PBANPs crystal nucleus growth is mainly controlled by thermodynamics. Therefore, the (100) facet with lower surface energy is thermodynamically more stable, which is also similar to the previously described growth induced by ethanol as a solvent. The cavity structure of Mn–Co–PBA greatly increases the rate of ion diffusion, making it an outstanding contender for biosensors.

With the gradual discovery of the application of PB as a biological material, some compounds can play the above roles, and are also endowed with better modification sites or provide targeting by themselves, bringing special responsive properties to PBNPs. Wang *et al.* prepared Mn–Co–PBA with a size of 150 nm by hydrothermal method using $MnCl_2$ as the Mn source and $CoCl_3$ as the Co source with PVP and $K_3[Fe(CN)_6]$.[86] Then, 1,2-dipalmitoyl-*sn*-glycero-3-phosphocholine (DPPC), dimethyldioctadecylammonium bromide (DODAB), and DSPE–PEG2000–Maleimide were prepared into liposomes under the condition of chloroform. PBS (pH 7.2) was used to replace the solvent, and then a stable solution was formed. Finally, $HAuCl_4$, ascorbic acid and liposome were added to the Mn–Co–PBA solution to grow gold nanoflowers on the surface of Mn–Co–PBA and form a liposome coating that could be described as LPBR. The LPBR can perform hyperthermia and controlled release of siRNA based on photothermal properties, and can perform PAI, CT, PTI multi-model imaging (Fig. 10E). The addition of liposomes will enable NPs to have more precise targeting, which will deepen the specific application of PBNPs in targeted therapy. Ran *et al.* physically encapsulated PBNPs using poly(lactic-*co*-glycolic acid) (PLGA) and tumor cell membranes in turn, and utilized the photothermal properties of PB to control the release of the loaded chemotherapeutic drug docetaxel (DTX) and immune adjuvant-imiquimo (R837).[132] The functional nanoparticles, in addition to their specific targeting, make

good use of the properties of PB for PA-MR guidance and monitoring during treatment (Fig. 10F). Emelianov *et al.* performed multimodal US/PA/MRI imaging with glucosinolate-modified PBNPs.[133] In their work, they achieved intraoperative real-time guided stem cell injection and postoperative monitoring of stem cell therapy in the spinal cord. Their research system demonstrated imaging several features of the method, proving that PBNPs are expected to play a key role in the treatment of bone marrow stem cells. In addition to providing targeting properties, the outer polymer coating can reduce the toxicity of other elements in the PB complex. Chen *et al.* applied PEI to self-assemble on PBNPs, and then used the amidation reaction and aldimine condensation to combine the Ce6 molecule and the aldehyde group of PEG with PB@PEI.[134] The outermost PEG coating can reduce the toxicity of nanoparticles. When the nanoparticles aggregated in the tumor area, under acidic conditions, the PEG was shed to expose the cytotoxicity of PEI and Ce to enhance the PDT effect. With the continuous expansion of the application range of PBNPs, the preparation technology of PB complexes is updated. The preparation of nanofiber materials by electrospinning technology is one of the most important academic and technical activities in the field of materials science and technology in the world in the past ten years. Lu *et al.* introduced Co–PBA into polyacrylonitrile (PAN) nanofibers by electrospinning, and then polymerized conductive polypyrrole nanotubes (PPy NTs) on their surfaces to prepare H–Co–PBA@PPy NTs.[2] The excellent electron transport properties with unique void confinement effect can be further applied to biosensors. The technology combines polymers with PB by electrospinning, which not only makes the polymer exist in a special way, but also promotes the combination of emerging technologies with the traditional preparation method. Choi *et al.* prepared PB-electrospinning nanofibers in another way, using the ROS scavenging power of PBNPs to demonstrate its good antioxidant and wound-healing properties.[135] In the study, chitosan of different molecular weights was used as dispersants to prepare PBNPs with a particle size distribution below 100 nm, and then their aqueous solutions were uniformly mixed with 10 wt% PVA aqueous solutions for electrospinning (Fig. 10H). The material could be used as an important part of the subsequent hydrogel wound dressing material – mechanical scaffolds, and the research further extended the application space of electrospinning technology and PBNPs as biomaterials. A PB composite microneedle was designed by Ji *et al.* with PVP/PVA as the base material, PCL as the needle, and PB as the responsive material for photothermal chemotherapy.[136] Among them, PBNPs of about 200 nm were first prepared by hydrothermal method, and then PB, Dox·HCl and PCL were uniformly mixed to prepare needles, and finally combined with the base solution of PVP/PVA (20 wt%/30 wt%) to form composite microneedles. During the application process, the PB will convert the light into local hyperthermia, and at the same time, the heat generated will dissolve the PCL for drug release. The work provides a minimally invasive strategy for hyperthermia-related multimodal therapy.

Initially, the polymer was only involved in the preparation of PBNPs with reducing agents and dispersants. With the continuous development of preparation technology, more polymers were added to the preparation of PBNPs in various identities and ways. With the modification of PBNPs with more novel polymer compounds, not only can their size be controlled or their properties (such as dispersion/crystallinity) be optimized to a certain extent, but PBNPs can also be functionalized to expand their biomedical application scope and diversify the application methods.

5.2 PB(PBA)/inorganic materials

First of all, both PBNPs and various PBAs are essentially MOFs of inorganic materials, and the modification of PBNPs by inorganic materials is often fundamentally different from that of organic materials. With the continuous development of PB-inorganic composite materials, some inorganic compounds with special properties have been gradually introduced into the preparation process, such as graphene, carbon nanotubes, and gold nanoparticles.[137–140] Some inorganic nanoparticles (nanospheres, nanostars, nanowires) introduced earlier can be prepared as templates.[141,142] When these templates are etched before application, the products can be classified as pure PBNPs, while the remaining templates can be classified as PBNPs doped with other elements or modified with inorganic materials. The size and pore controllability of PBNPs often make it possible to load some suitable nanoparticles for synergistic effect. For example, PBNPs-loaded gold nanoparticles can enhance the photothermal effect for photothermal therapy. Another inorganic material modification is the formation of nanoshells on the outside. It is known from the published research reports that most of the inorganically modified PBNPs and PBAs exist in the form of load and core–shell, and their products have been obtained for the specific properties of PTT, PDT, biosensing, ROS detection and bioimaging optimization. At first, the composite materials formed by the addition of gold nanoparticles in the PB preparation process only served as templates or provided photothermal properties. With the deepening of the research on PB and nano-gold, the application scope of such composite materials has also expanded. Zhang *et al.* used the AuNWs with an average length of 7.0 μm as the substrate to grow PB on its surface with dual precursors. The resulting product solution was dropped on the bare glassy carbon electrode (GCE) to form PBNPs@AuNWs/GCE with improved electrical conductivity and electron transport capability, which can be used to detect H_2O_2 in human serum samples and HeLa cells.[143] The allied core–shell structure was formed as Dai *et al.* took advantage of the high X-ray absorption coefficient of gold nanoparticles and loaded them with PBNPs to form Au@PB NPs core/shell NPs of around 10 nm.[144] Combining the properties of PBNPs and AuNPs, CT imaging and photoacoustic (PA) imaging can be performed (Fig. 11A). The magnetic properties of PB with conventional size are weak. Due to the continuous design of PB complexes with core–shell structure, some researchers use iron oxide or other compounds with better magnetic properties as the core or shell to form complexes to improve the magnetic properties. Li *et al.* first prepared ultra-small Fe_3O_4 NPs by co-precipitation method, and then added $K_4[Fe(CN)_6]$ solution and

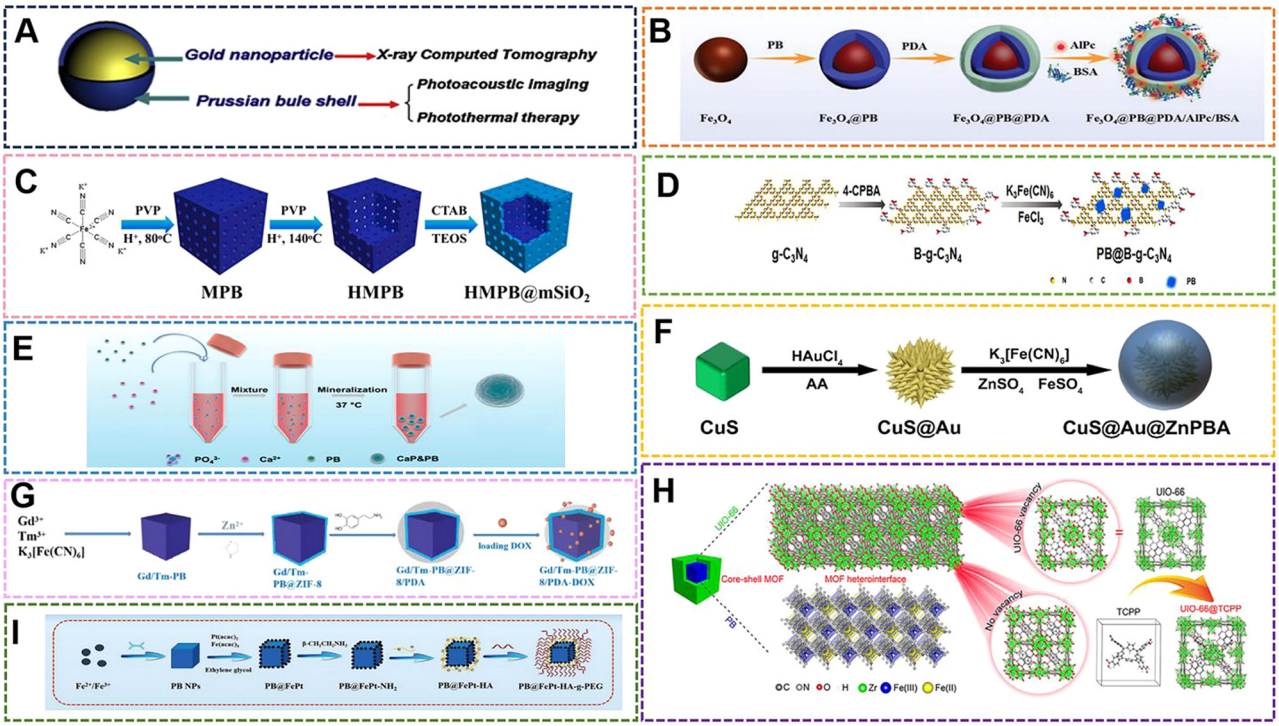

Fig. 11 (A) Structural and functional illustration of Au@PB NPs. Reprinted from ref. 144 with permission. Copyright 2014 Elsevier. (B) Structural of Fe_3O_4@PB@PDA/AlPc/BSA nanocomposites. Reprinted from ref. 145 with permission. Copyright 2018 Royal Society of Chemistry. (C) Schematic depiction of preparation HMPB@mSiO2. Reprinted from ref. 146 with permission. Copyright 2022 Elsevier. (D) The preparation of PB@B–g-C_3N_4 nanohybrids. Reprinted from ref. 147 with permission. Copyright 2022 Royal Society of Chemistry. (E) Schematic of the mineralization process of PBNPs. Reprinted from ref. 148 with permission. Copyright 2022 Royal Society of Chemistry. (F) Schematic representation of the fabrication of the CuS@Au@ZnPBA NPs. Reprinted from ref. 149 with permission. Copyright 2022 Elsevier. (G) Schematic illustration of the synthetic procedure of Gd/Tm–PB@ZIF-8/PDA. Reprinted from ref. 151 with permission. Copyright 2020 Royal Society of Chemistry. (H) Schematic illustration of the core–shell structure of PB@MOF. Reprinted from ref. 152 with permission. Copyright 2019 American Chemical Society. (I) Schematic representation of the fabrication of the PB@FePt NCs. Reprinted from ref. 153 with permission. Copyright 2020 Royal Society of Chemistry.

$FeCl_3$ aqueous solution to Fe_3O_4 NPs aqueous solution under stirring at room temperature. The PB nanoshells were then mixed under the acidic condition of the reaction system. Fe_3O_4@PB NPs were formed by deposition onto Fe_3O_4 nanocores. Finally, Fe_3O_4@PB NPs were coated with polydopamine (PDA)/aluminum phthalocyanine (AlPc)/bovine serum albumin (BSA), making it a promising candidate for MR/PA/NIRF bioimaging-guided magnetic targeting synergistic therapy for cancer nanoplatform.[145] Among them, the Fe_3O_4 core has magnetic targeting and T_2-weighted MR imaging, while the PB shell can be used as a probe for photothermal agent and photoacoustic (PA) imaging, which can make up for the lack of MRI in deep tissue signal. AlPc can be used for PDT and NIR fluorescent imaging agent with the advantages of high specificity and simple operation. Meanwhile, the presence of BSA acts as a surface stabilizer, which prolongs the circulating half-life of the nanoparticles. However, the platform, as a multimodal imaging tool, has an obvious effect on PTT treatment under NIR irradiation, and AlPc can be absorbed by PDA and combined with BSA, thereby promoting the absorption of AlPc by cells (Fig. 11B). In addition to this, PB can appear in the complex as a nucleus. Li *et al.* prepared a hollow structure drug carrier with photothermal response and high drug loading rate, HMPB@$mSiO_2$ with HMPB as the core and silica coating as the shell induced by CTAB[146] (Fig. 11C). This involved the same way to grow PBNPs after selection as Xu's research group. They prepared PB-B–g-C_3N_4 by simply mixing boronic acid-modified graphite carbon nitride (g-C_3N_4), $FeCl_3$ and $K_3Fe(CN)_6$ for Raman recognition of SA on cancer cells, and synergistically enhanced PTT/PDT.[147] PB grows on C_3N_4, and the large surface area of B–g-C_3N_4 increases the contact with the surrounding O_2. This leads to the rapid and abundant generation of ROS, thereby improving the therapeutic efficiency (Fig. 11D). In order to enhance the photothermal properties, Kong *et al.* introduced the technology of biomineralization into the preparation process of PB. They utilized the interaction between PB and calcium ions to confer the as-prepared PBNPs with $CaCl_2 \cdot 4H_2O$ at 37 °C for 60 min to obtain biomineralized PB (CaP-PB).[148] The induction of calcium in the structure can narrow the band gap of PNNPs, thereby improving the photothermal conversion efficiency (PCE) of PBNPs (Fig. 11E). With the continuous development of PB core–shell nanoparticles, multilayer core–shell structures have also been designed. Hu *et al.* used CuS NPs as the core to sequentially grow Au NPs and Zn–PBA NPs on its outside to form a composite structure of CuS@Au@Zn–PBA with a size of 200 nm, which assisted the Zn–PBA antibacterial through the LSPR coupling effect between CuS and Au[149] (Fig. 11F).

There is another special material in the modification by inorganic materials, in which the framework of PB is modified by other MOFs.[15,150] MOFs are covalently bonded by metal ions

and organic ligands, and their framework structures have excellent chemical stability in most solvents. MOFs have flexible structural characteristics, which will change with some external factors, such as the existence of guest molecules, temperature and pressure. Therefore, this also provides a strong basis for composite compounds, such as MOF@MOF. Generally, most of the PBNPs combined with other MOFs are grown on one outer surface and another, and the core–shell structure is formed when the outer MOFs are grown uniformly. Wang *et al.* used $Gd(NO_3)_3{\cdot}6H_2O$ as the gadolinium source, $TmCl_3{\cdot}6H_2O$ as the thulium source, and $K_3[Fe(CN)_6]$ by solvothermal method to prepare 200 nm Gd–Tm–PBA at 140 °C.[151] Then, ZIF-8 was grown *in situ* on its surface by solvent method again to synthesize Gd–Tm–PBA@ZIF-8. Finally, the composite form of Gd–Tm–PBA@ZIF-8@PDA was formed by external coating with dopamine. The structure has excellent magnetic properties, fluorescence effect, photothermal properties, and drug loading capacity, so that it can implement fluorescence imaging (FOI), magnetic resonance imaging (MRI) tracking, and photothermal–photothermal synergistic therapy (Fig. 11G). Such external modification caused PDA and ZIF-8 to become two drug-loaded valves, which can realize GSH/pH dual-triggered relative chemotherapy under certain conditions. In addition to the formation of specific MOF shells, organic ligands in MOFs can enhance the performance of PBNPs to a certain extent. Wu *et al.* used PB as the core to grow porphyrin-doped UIO-66 externally to form the structure of PB@UIO-66. The two-step crystal growth methods were hydrothermal method and solvothermal method.[152] Porphyrin doping can compensate for the defects in UIO-66 and enhance the transfer of photoexcited electrons from PB, thereby enhancing the yield of singlet oxygen and enhancing the nanoenzyme activity. PB@UIO-66 produces outstanding antimicrobial properties under dual irradiation with 808 nm NIR or 660 nm red light (Fig. 11H).

In recent years, a new way to prepare PB-inorganic composites has been developed, which is to *in situ* grow nanodots of other functional elements on the surface of PBNPs. This approach differs from the above-mentioned core–shell structures in that ultra-small-sized nanodots are randomly distributed on the surface, but do not form a dense or particle network shell. Under such a structure, the compound maintains the structure and morphology of PB to the greatest extent, and at the same time reduces the weakening of some physicochemical properties after modification. In this way, Zheng *et al.* constructed a multifunctional tumor treatment system based on PBNPs, which integrates diagnosis and treatment, realized PDT/PTT synergistic therapy, and performed MR/CT/PI triple imaging.[153] During the preparation of the material, PBNPs were first obtained by mixing $FeCl_3$, $K_4[Fe(CN)_6]$ and citric acid by co-precipitation method, and then the reduced FePt NPs could be effectively anchored by monodentate bonds (–COO–Fe–) on the surface of PB NCs. Their data indicate that the PB@FePt-HA-g-PEG NCs composite nanomaterials prepared in the work have excellent therapeutic effect on 4T1 cells (Fig. 11I). Similarly, Zhang *et al.* reduced H_2PtCl_6 on PBNPs of around 100 nm to obtain Pt–PBAs with different doping contents.[154] It can be seen from multiple data that the structure and morphology of Pt–PBA do not change significantly, but the black spots on the surface increase with the increase of Pt content. The Pt content affects the change of the band gap, and then increases the electronic transition circuit path. Thus, Pt–PBA has a tunable LSPR frequency to suit special clinical needs and increase the application wavelength range. Furthermore, the photothermal conversion efficiency of Pt–PB was increased from 32.5% to 58.2%. Original photothermal agents can only perform photothermal conversion in a specific frequency range. With the continuous updating of therapeutic instruments and methods, photothermal agents with tunable controllability in complex clinical needs are being developed and designed (Tables 1 and 2).

With the continuous development of the preparation technology of PBNPs and PBAs, the basic structure modification of PBNPs and PBAs by other inorganic biomaterials will further expand the application scope as biomaterials. In the early stages, the modification of PB by MOFs is mostly in the form

Table 1 Summary of PBNPs for different preparation methods (D-dual-precursor /S-single-precursor)

Preparation method	Reaction temperature	Reaction time	Particle size	Morphology	Synthetic strategies	Ref.
Coprecipitation	RT	0.1 h	16 nm	Cubic	D	34
Microemulsion	RT	72 h	160 nm	Nanoboxe	D	41
Microemulsion	RT	48 h	250 nm	Cubic	D	42
Microemulsion	RT	0.5 h	34 nm	Cubic	D	8
Microemulsion	80 °C	0.5 h	75 nm	Spheric	D	167
Hydrothermal	140 °C	8 h	60 nm	Nanosheet	D	48
Hydrothermal	60 °C	0.5 h	70 nm	Cubic	D	50
Hydrothermal	80 °C	20 h	110 nm	Spheric	S	11
Hydrothermal	140 °C	4 h	80 nm	Cubic	S	100
Hydrothermal	80 °C	20 h	100 nm	Cubic	S	109
Hydrothermal	80 °C	12 h	150 nm	Spheric	S	164
Template-assisted method	RT	—	25 nm	Spheric	D	57
Template-assisted method	RT	4 h	140 nm	Nanoshell	D	59
Solvothermal	80 °C	3 h	3.4 nm	Spheric	S	66
Solvothermal	80 °C	4 h	200 nm	Nanoflower	S	67
Sonochemical method	40 °C	5 h	250 nm	Cubic	S	70
Magnetic internal heating	80 °C (11.5 A)	0.5 h	5 nm	Cubic	S	72
Gas shearing method	RT (1 mL h^{-1})	—	300 nm	Spheric	D	73

of surface growth and composite compounds in the form of PB@MOFs or MOFs@PB, which have the properties of combining two or more materials, and these properties can have a synergistic effect. The structure may also have different properties due to interfacial heterogeneity, but some core–shell structures often also have some excellent properties that shield or weaken the core. Therefore, such modifications should precisely control the growth length of the outer material and the choice of the inner and outer shells, according to the application direction. However, some researchers recently chose to grow on the surface of PBNPs in a "dispersed" way, which better maintains the morphology of PB compared with the core–shell structure, and has almost no shielding effect. This preparation technique is also expected to be more widely used in the modification design of PB by other inorganic compounds.

5.3 PB(PBA)-functionalized hydrogel materials

In the field of bio-nanomaterials, hydrogel materials are an indispensable part. The hydrogel is a kind of polymer material with a unique three-dimensional network structure. Because of its good biocompatibility, sensitivity to the environment, abundant sources, and low price, the hydrogel has become a major research topic as a biomaterial in recent years. Hydrogels typically exist in the form of gels, injectable gels, microgels and nanogels.[155–157] Gels are often used in wound dressings, vascular stents, tissue adhesion, and cardiac patches in the biomedical field.[158–161] Injectable hydrogels are also used as carriers to load drugs for sustained and controlled drug release, targeted release, or loaded with nanoparticles for diagnosis and treatment of tumors. While microgels and nanogels are polymers with a size in the range of 1–1000 nm, and are cross-linked and polymerized within the molecule, they have wider applications in diagnostic analysis and regulation of enzyme activity due to their smaller size. As a multifunctional biomaterial, the combination of PB with hydrogel materials will further expand and extend the development of PB in many application directions, and its research has great application value. This synthesis not only focuses on size and fundamental properties, but also combines it with other polymers or materials, such that different chemical components meet at the interface of nanoparticles and other polymers or compounds. From the development of nanomaterials, these materials integrate multiple properties of PBNPs and specific polymer compounds in a single system, and exhibit excellent response properties in different application environments.

PB-based hydrogels usually refer to PB or PBA as an important component of hydrogels, or to provide support for the gel network, or to provide some special properties for gel applications. There are three ways to participate, one of which is the simplest PBNPs as inorganic nanoparticles doped in the hydrogel synthesis process. This method is the simplest, and the hydrogel is usually prepared by a one-pot method. When selected, the selectivity of the preparation method of PBNPs can be more diverse, the concentration of nanoparticles can be accurately determined, and the peripheral modification compounds of PB can be selected at the same time. The most important is that the size of PB is precisely controlled. Another way is to first select the iron source, add the iron source during the preparation of the gel, and control the temperature, pH, and reaction time to perform the *in situ* synthesis of PB inside the gel under the conditions of gel preparation. In this way of participation, PB can better connect with the gel network, and can even form covalent bonds for linking. The further connection with the gel network can also allow PB to control the gel network to a certain extent, which makes PB-based hydrogels more flexible and diverse in application. Although this method is more flexible in application, it still has great limitations in preparation technology. For example, the pH value of PBNPs preparation conditions limits many polymer compounds to a large extent, and the preparation temperature also has the same effect, which will limit the addition of some protein molecules to a certain extent. Thus, the preparation of PB-based hydrogels by *in situ* synthesis is greatly limited in the selection of materials, and this gel preparation technology has much room for improvement. The last way is to use Fe(III) in PB or to exploit the groups on some polymer short chains in the preparation process (such as redundant unmodified amino, carboxyl and aldehyde groups) to link the compounds that form the gel network by covalent bonds or non-covalent bonds. This method is milder than the above two methods. On the one hand, the PBNPs can be prepared first, according to the need to prepare PB or PBA of different sizes. On the other hand, compared with *in situ* synthesized PB-based hydrogels, it has almost no limitations in the selection of macromolecular compounds that are important components of the gel network. In some gel networks, its covalent or non-covalent bonds with polymer segments can impart more properties to the network.

Table 2 Summary of PBA for different elements and their application

Framework elements	Application	Year	Ref.
Co	PTT, PDT/PTT, PAI, CT	2021/2020	85,131
Zn	PTT, PDT/antibacterial/PTT, drug carrier/antibacterial, PTT	2019/2022/2022/2022	86,88,89,149
Mn	Catalytic/nanoenzyme/PTT, PAI, CT	2016/2022/2020	91,113,131
Cu	PTT, PDT	2021	90
Ga	PTT, PAI, CT, PTI/MRI, PA, PTT/drug carrier, MRI	2022/2016/2020	86,92,151
Ag	Anticancer, antibacterial	2020	87
Mo	PTT	2019	93
Yb	PTT, PAI, CT, PTI	2022	86
Tm	PTT, PAI, CT, PTI/drug carrier, MRI	2022/2020	86,151
Cd	Catalytic	2020	114
Bi	Nanoenzyme/nanoenzyme	2022/2019	16,115

The easiest way to prepare PB-based hydrogels is to prepare PBNPs at first. The PBNPs solution was then uniformly mixed with the gel pre-preparation solution and distributed throughout the system before the gel network was formed. For example, Piersandro Pallavicini *et al.* selected the co-precipitation method to prepare PBNPs by $FeCl_3$ and $K_4[Fe(CN)_6]$, and then used PVA and PEG-200 as monomers, PBNPs as a physical adsorption cross-linking agent, and then gelation was carried out by means of freezing cycle.[162] The product PB-PVA hydrogel films had certain antibacterial properties due to the photothermal properties of PBNPs. However, one weakness of the paper is that the simplest PBNPs are used alone and the surfaces are not modified by other polymers, so it cannot form a large number of hydrogen bonds with the PVA segment. Furthermore, only simple physical forces exist, resulting in poor mechanical properties of the hydrogel. Using the same preparation strategy, Wang *et al.* combined PBNPs with PEDOT:PSS conductive hydrogels for non-invasive and continuous monitoring of glucose on the body.[163] In the porous three-dimensional network of the hydrogel, the internal PBNPs will provide a large number of electron transport paths and abundant active sites to functionalize the hydrogel. The study demonstrated that PBNPs also have great potential in hydrogel biosensing. The addition of PBNPs as MOFs can provide hydrogels with poor electrical conductivity, better electrochemical performance, enhancing their electron or proton transport effect, and make them applicable in wearable sensors, ionic skin, and specific biomonitoring (Fig. 12A).

Due to the versatility of PBNPs in the biological field, PB-based hydrogels generally retain most of the excellent properties of PB. These properties are often combined with the gel monomer material, making it better for applications. Du and his team exploited the photothermal properties of PB to design an injectable hydrogel containing PB nanospheres for photothermal therapy.[164] In the work, a commercially available thermosensitive hydrogel-Pluronic F127 was selected for coating, wherein the gel was liquid when the temperature was higher than the phase transition temperature of 41 °C, and semi-solid when it was lower than the temperature point. The gel has excellent photothermal conversion ability and photothermal repeatability. As a new PB-based hydrogel applied as a photothermal agent, it exhibits good photothermal effect. With the same use of

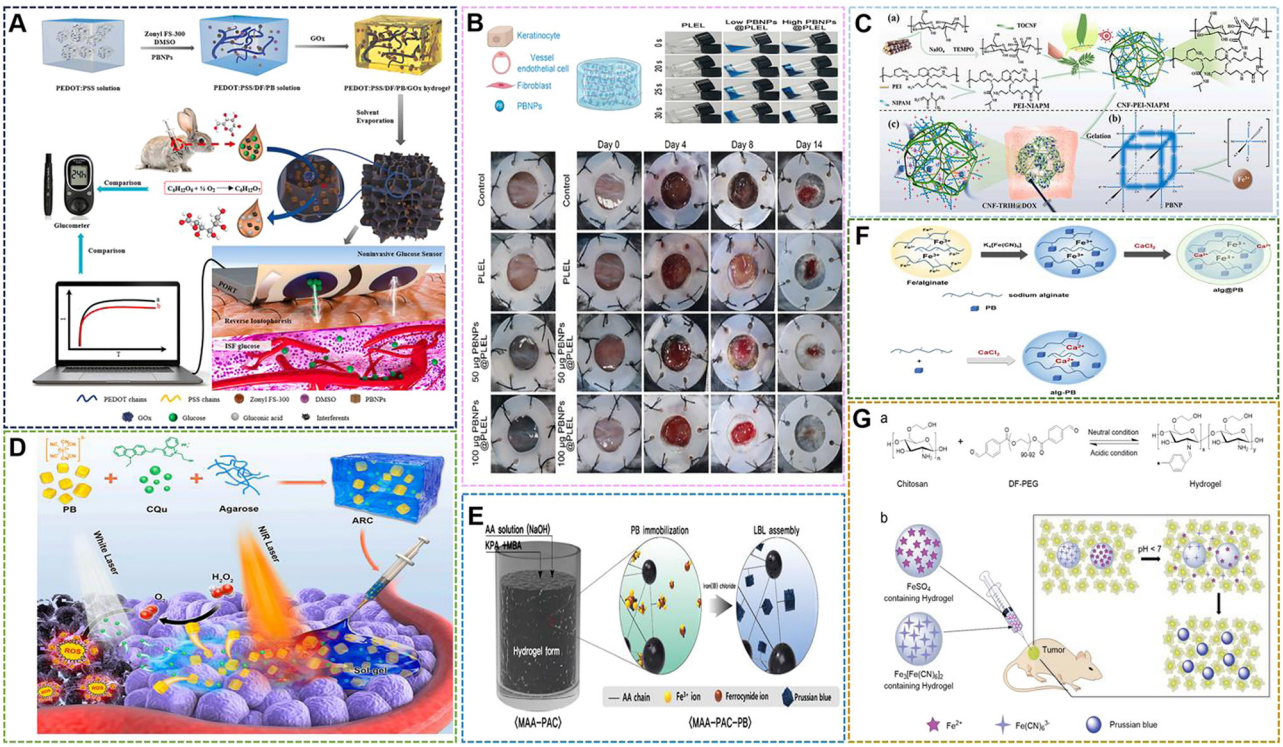

Fig. 12 (A) The schematic demonstration on the preparation of PEDOT:PSS/DF/PB/GOx sensor for the glucose detection in serum and the noninvasive ISF glucose detection on human skin based on the reverse iontophoresis (RI), along with comparison to the glucose measurement by commercial glucometer. Reprinted from ref. 163 with permission. Copyright 2022 Elsevier. (B) Schematic overview of the use of PBNPs@PLEL for the enhancement of diabetic wound healing owing to their ability to scavenge ROS and to promote the functional recovery of mitochondria. Reprinted from ref. 167 with permission. Copyright 2022 American Chemical Society. (C) The synthetic route of CNF-PEI-NIPAM (a); the synthetic route of PBNPs (b); the synthetic route of CNF-TRIH@DOX(c). Reprinted from ref. 165 with permission. Copyright 2022 Elsevier. (D) Schematic illustration of an injectable nanozyme hydrogel as AIEgen reservoir and release controller for efficient tumor therapy. Reprinted from ref. 166 with permission. Copyright 2021 Elsevier. (E) Scheme for the hydrogel by polymerization of acrylic acid and immobilization of PB by LBL assembly. Reprinted from ref. 169 with permission. Copyright 2019 Nature. (F) Schematic illustration of the formation of sodium alginate-based composite beads in which PB was chemically-bound (alg@PB) and was simply-embedded (alg-PB). Reprinted from ref. 168 with permission. Copyright 2018 Elsevier. (G) Schematic illustration of (a) formation of pH-responsive hydrogel, and (b) *in situ* formation of PB in the tumor area. Reprinted from ref. 170 with permission. Copyright 2017 Royal Society of Chemistry.

photothermal properties, He *et al.* used citric acid as a surface capping agent to enhance the colloidal stability of PBNPs prepared by $FeCl_3$ and $K_4[Fe(CN)]_6$ (Fig. 12C). They selected CNF–PEI–NIPAM as the temperature and pH-responsive material. The PBNPs finally combined with sodium alginate and chitosan to form a novel temperature, pH and NIR tristimulus responsive Inject hydrogel with nanocages and 3D network structures.[165] PBNPs act as a switch for photothermal response in the gel system. In the three-dimensional network of the hydrogel, the way of physical doping can also exert the enzymatic activity of PB. Tang *et al.* developed a novel injectable nanoenzyme hydrogel using agarose as the gel monomer, which acts as an AIEgens reservoir and release controller (ARC) to facilitate more effective tumor therapy.[166] The ARC system is achieved by simultaneously encapsulating PBNPs and AIEgen (CQu) in agarose hydrogels. The gel can generate high levels of reactive oxygen species and sufficient oxygen after *in vivo* injection to induce cytotoxicity of tumor cells, exhibiting good antitumor efficacy under its therapeutic regimen (Fig. 12D).

Another main application direction of the composite material combined with PB and hydrogel is wound dressing, and the hydrogel can be used as a drug delivery system as a wound dressing. Meanwhile, the 3D network porous structure and high water content of the hydrogel can play the role of promoting oxygen exchange, absorbing exudate and maintaining water balance. The addition of PBNPs can give full play to their nanoenzyme properties. This is because being encapsulated in the gel network can effectively scavenge ROS for a long time and promote wound healing. Chen *et al.* prepared thermosensitive poly(D,L-lactide)–poly(ethylene glycol)–poly(D,L-lactide) (PDLLA–PEG–PDLLA) hydrogels physically doped with PBNPs ((PBNPs@PLEL)). The results indicated that PBNPs@PLEL could promote skin wound healing in diabetic mice, exhibiting good ROS scavenging ability and anti-inflammatory effect[167] (Fig. 12B).

The *in situ* growth of PBNPs in the hydrogel system can not only functionalize the hydrogel, but also enhance the hydrogel network by regulating the size of the PB and exploiting the vacant sites in the structure. Lee *et al.* successfully prepared a new type of sodium alginate-PB composite hydrogel using the original synthesis method. In the gel network, the algae was first mixed with Fe(III) solution to form the Fe(III)-alg gel composite after washing the beads. $K_4[Fe(CN)_6]$ was then added, and the gel immediately changed from yellow to blue, forming PB-alg gel composite beads.[168] Among them, Fe(III) first acts as a cross-linking agent in sodium alginate gel, and has two roles of cross-linking agent and reactant in the process of PB synthesis (Fig. 12F). In the research study, the direct physical doping of sodium alginate gel with PBNPs was also compared, and the data showed that the common physically doped PB partially aggregated inside the gel, while the *in situ* synthesis method had a more uniform distribution of PB and large amounts of PBNPs can be introduced. Therefore, the chemical *in situ* synthesis shows obvious advantages in PB loading efficiency. Using the similar growth pattern of PB, Hwang *et al.* designed a hydrogel MAA-PAC impregnated with powdered activated carbon (PAC) through the polymerization of acrylic acid (AA) to develop an adsorbent with enhanced PB content and immobilization stability.[169] The addition of powdered activated carbon (PAC) enhanced the mechanical strength of the gel. Fe(III) was first adsorbed by MAA-PAC, and the supply of Fe^{3+} ions was provided by layer by layer (LBL) assembly, followed by the addition of potassium ferrocyanide solution (Fig. 12E). PB particles grew and were stably immobilized. At the same time, the carboxyl groups of AA immobilized PB. This move is also used in *in situ* synthesis. At the same time, it also utilizes the spare Fe(III) sites in the structure to combine with AA, effectively immobilizing PB in the gel. Most of the existing studies use gels as carriers to deliver prepared PBNPs into the body. However, Wu *et al.* constructed an intelligent therapeutic system with pH-responsive triggering of PB, which exhibited excellent performance in the PAI-guided photothermal therapy of PTT tumors.[170] The system is to encapsulate ferrous ions and ferricyanide ions separately with pH-responsive injectable hydrogels. When the gels are injected into tumor-bearing mice under acidic conditions near the tumor, the gels will degrade to release the required PB synthesis precursors to form PBNPs (Fig. 12G). The *in situ* formation of PBNPs at the tumor site enhanced PAI imaging to some extent, and photothermal therapy could be introduced.

Although some research progress has been made in the synthesis of several PB-based hydrogels, and their research products have obtained certain application value or research significance in various fields, most of the PB-based hydrogels are based on simple physical doping preparation. The *in situ* synthesis and gel modification processes are rarely reported, and these two methods are likely to become new ways to open PB-based hydrogels, which is expected to make PB. The application of PB-based hydrogels in the field of biomedical materials has taken an important step, so it has great application potential and research significance to explore the preparation of PB-based hydrogels in these two ways.

6. Summary and outlook

In general, with the continuous exploration of PBNPs as biomedical materials in various fields, the preparation technology of PBNPs has gradually shifted from the methods of traditional hydrothermal and co-precipitation to more controllable methods, such as emulsion polymerization, solvothermal and magnetic internal heating method. However, in the process of continuous development and optimization of preparation methods, in addition to the effect and yield brought by the properties, one should also focus on the biosafety, continuous preparation, and structural flexibility. Although some of the existing novel preparation methods have been developed and designed, the mechanism of the growth and formation of PBNPs still need to be further improved.

The structure of PBA is similar to PB. Therefore, most of the various PBAs have the same results that PB has achieved in many fields, or the application potential in the field of biomedicine. Divided from the introduction of elements or ions, PBA

can be divided into two categories from the material structure. The first type is to modify the framework structure by introducing other metal elements (*e.g.*, Co, Mn, Ni, Cr, Ga, Bi) to form PBA. Part of the elemental replaceability in the PB framework as a classic metal–organic framework endows PBA with multiple possibilities as biomaterials. For example, the introduction of elements (such as Ag, Mo, Bi, and Cu) into the structure would make the formed PBA a novel near-infrared-II activated inorganic photothermal nanomedicine. The introduction of Ga and Mn elements would enhance the effect of NMR imaging, photothermal and photoacoustic imaging of PBA. At the same time, the introduction of Co, Se and other elements in the framework would improve the properties of MRI, enzyme-like activity, and ROS scavenging effect. The second type is by changing the interstitial ions in PB, such as Na^+, K^+, Rb^+, and Cs^+, which are usually used in the optimization of electrochemical properties. At present, these materials are only studied in the direction of electrodes and capacitors. With the development of wearable sensor devices in recent years, hydrogels and a number of polymer films have become the research hotspots for such materials. The internal ion-modified PBA has excellent electrochemical properties, which can be combined with the hydrogel or polymer film through physical doping, *in situ* growth, and chemical bonding, and is expected to form a new generation of flexible wearable sensor devices. There is a different strategy for modifying PBNPs to endow PB with excellent dispersibility, biocompatibility and targeting by modifying external compounds with hydroxyl, amino and carboxyl groups. With the continuous optimization of preparation technology and application methods, polymer compounds not only play the role of initial dispersants, reducing agents and protective agents, but the PBA formed by the addition of some polymer compounds is also destined to bring rich special sites. At the same time, it can also express the absorption, circulation, distribution and metabolism of nanoparticles *in vivo*, as well as improve immune escape and avoid immune clearance. For example, micellar or nanogels are used to encapsulate drug-loaded PBNPs for selective release by changing the external environment. The compounds (such as dopamine, cyclodextrin and liposome) can also be selected to add targeting sites. Some of the organic compounds can be selected to enhance the absorption of materials in the second near-infrared region to enhance the therapeutic effect. These modified and optimized PBAs would further expand its application in the field of diagnosis and treatment. Another strategy to modify PBNPs is to form a core–shell structure with some inorganic nanoparticles or to dope or support/support inorganic nanoparticles as templates. The addition of Fe NPs or Cu_2S nanoparticles can improve the properties of PBA, such as MRI imaging, enzyme-like activity, and ROS scavenging effect. The addition of Au NPS, Ag NPs and other particles or the formation of Au and Ag core–shell structures would enhance the photothermal properties of PBA. In addition, some multifunctional nanodots can also be applied to grow uniformly on the PB surface. For example, Pt, Cu_2S, Au, Ag, and others improve the photothermal properties. Oxides are also a good modification scheme for PBA. Part of the oxides can be combined with Fe^{3+} in the vacancy of the PB structure, so as to exist stably and exert specific biological characteristics. Compared with other methods, the modification of inorganic materials is more controllable in terms of the preparation technology, and its distribution and content are more definite in terms of structure.

Therefore, although a large number of PB and PBA derivatives have been developed and studied, it is necessary to further optimize their preparation methods and application mechanisms to design and explore new structural PBA or PB(PBA) composites as biological materials, which have great research significance and clinical application potential. This kind of work will continue to become a research hotspot in the near future. It has emerged in many biomedical fields. The research and treatment of integrated multifunctional PB nanomaterials have great potential to solve important biomedical problems. This opens up a class of safer and more effective materials for the research of medical diagnosis and treatment, playing an important role in the on-site instant diagnosis of diseases and cancer treatment, and promotes the development of medical diagnosis and treatment and clinical applications based on nanomaterials.

Conflicts of interest

There are no conflicts to declare.

Acknowledgements

This work was supported by the National Natural Science Foundation of China (51832001 and 61821002), and the Nanjing Science and Technology Development Foundation (202205066).

References

1 N. Song, S. Ren, Y. Zhang, C. Wang and X. Lu, *Adv. Funct. Mater.*, 2022, **32**, 1032–1040.
2 G. Tian, X. Ran, Q. Wang and D. Zhang, *Dalton Trans.*, 2022, **51**, 1032–1040.
3 M. Eryiğit, E. P. Gür, M. Hosseinpour, T. Ö. Özer and H. Ö. Doğan, *Mater. Today: Proc.*, 2021, **46**, 6991–6995.
4 G. Zhang, Y. Li, X. Xiao, Y. Shan, Y. Bai, H. G. Xue, H. Pang, Z. Tian and Q. Xu, *Nano Lett.*, 2021, **21**, 3016–3025.
5 S. Kaye and J. Long, *J. Am. Chem. Soc.*, 2005, **127**, 6506–6507.
6 J. Peng, W. Zhang, J. Wang, L. Li, W. Lai, Q. Yang, B. Zhang, X. Li, Y. Du, H. Liu, J. Wang, Z. Cheng, L. Wang, S. Wang, J. Wang, S. Chou, H. Liu and S. Dou, *Adv. Energy Mater.*, 2021, **11**, 6506–6507.
7 A. Takahashi, H. Tanaka, K. Minami, K. Noda, M. Ishizaki, M. Kurihara, H. Ogawa and T. Kawamoto, *RSC Adv.*, 2018, **8**, 34808–34816.
8 H. Pang, C. Tian, G. He, D. Zhang, J. Yang, Q. Zhang and R. Liu, *Nanoscale*, 2021, **13**, 8490–8497.
9 K. Zhang, J. Wu, X. Zhao, J. Qin, Y. Xue, W. Zheng, L. Wang, H. Wang, H. Shen, T. Niu, Y. Luo, R. Tang and B. Wang, *ACS Nano*, 2021, **15**, 19838–19852.

10 H. Bai, T. Wang, F. Kong, M. Zhang, Z. Li, L. Zhuang, M. Ma, F. Liu, C. Wang, H. Xu, N. Gu and Y. Zhang, *Chem. Eng. J.*, 2021, **405**, 126891.
11 X. Ma, J. Hao, J. Wu, Y. Li, X. Cai and Y. Zheng, *Adv. Mater.*, 2022, **34**, e2106723.
12 S. Ohkoshi, T. Iyoda, A. Fujishima and K. Hashimoto, *Phys. Rev. B: Condens. Matter Mater. Phys.*, 1997, **56**, 11642.
13 M. Okubo, D. Asakura, Y. Mizuno, T. Kudo, H. Zhou, A. Okazawa, N. Kojima, K. Ikedo, T. Mizokawa and I. Honma, *Angew. Chem., Int. Ed. Engl.*, 2011, **50**, 6269–6273.
14 S. Mallakpour, E. Nikkhoo and C. M. Hussain, *Coord. Chem. Rev.*, 2022, **451**, 214262.
15 H. Xu, K. Ye, K. Zhu, Y. Gao, J. Yin, J. Yan, G. Wang and D. Cao, *Inorg. Chem. Front.*, 2021, **8**, 2788–2797.
16 C. Ye, W. Zhang, Y. Zhao, K. Zhang, W. Hou, M. Chen, J. Lu, J. Wu, R. He, W. Gao, Y. Zheng and X. Cai, *Adv. Healthcare Mater.*, 2022, **11**, e2200787.
17 W. Zhang, J. Wang, Z. Xie, H. Zou, Q. Chen, L. Xu, L. Hu, N. Fang, J. Xu, J. Zhou, J. Liu, H. Ran, Z. Wang, Y. Zhang and D. Guo, *Small*, 2022, **18**, e2106252.
18 M. Kim, J. H. Lee and J. M. Nam, *Adv. Sci.*, 2019, **6**, 1900471.
19 X. Dai, X. Zhao, Y. Liu, B. Chen, X. Ding, N. Zhao and F. J. Xu, *Small*, 2021, **17**, e2006004.
20 N. M. Cativa, I. E. dell'Erba, C. V. Waiman, G. F. Arenas, M. Ceolin, L. J. Giovanetti, J. M. Ramallo-Lopez, G. Elicabe and C. E. Hoppe, *Langmuir*, 2020, **36**, 13998–14008.
21 X. Du, C. Zhao, M. Zhou, T. Ma, H. Huang, M. Jaroniec, X. Zhang and S. Z. Qiao, *Small*, 2016, **13**, 1602592.
22 M. Jeyaraj, S. Gurunathan, M. Qasim, M. H. Kang and J. H. Kim, *Nanomaterials*, 2019, **9**, 1719.
23 G. Gao, X. Sun and G. Liang, *Adv. Funct. Mater.*, 2021, **31**, 2100738.
24 G. Fu, W. Liu, S. Feng and X. Yue, *Chem. Commun.*, 2012, **48**, 11567–11569.
25 T. Uemura and S. Kitagawa, *J. Am. Chem. Soc.*, 2003, **125**, 7814–7815.
26 Z. Jia and G. Sun, *Colloids Surf., A*, 2007, **302**, 326–329.
27 Q. Zhang, L. Zhang and J. Li, *Electrochim. Acta*, 2008, **53**, 3050–3055.
28 R. Hou, T. Lu, W. Gao, J. Shen, Z. Yu, D. Li, R. Zhang, Y. Zheng and X. Cai, *ACS Nano*, 2022, **16**, 9559–9571.
29 J. Maer, M. Beasley, R. Collins and W. Milligan, *J. Am. Chem. Soc.*, 1968, **90**, 3201–3208.
30 X. Wu, M. Cao, C. Hu and X. He, *Cryst. Growth Des.*, 2006, **6**, 26–28.
31 B. W. Chen, Y. C. He, S. Y. Sung, T. T. H. Le, C. L. Hsieh, J. Y. Chen, Z. H. Wei and D. J. Yao, *Sci. Technol. Adv. Mater.*, 2020, **21**, 471–481.
32 Z. Chen, B. Fei, M. Hou, X. Yan, M. Chen, H. Qing and R. Wu, *Nano Energy*, 2020, **68**, 471–481.
33 S. Huang, X. Kou, J. Shen, G. Chen and G. Ouyang, *Angew. Chem., Int. Ed. Engl.*, 2020, **59**, 8786–8798.
34 F. Shiba, M. Nito, K. Kawakita and Y. Okawa, *Part. Sci. Technol.*, 2015, **33**, 671–676.
35 M. Shokouhimehr, E. S. Soehnlen, J. Hao, M. Griswold, C. Flask, X. Fan, J. P. Basilion, S. Basu and S. D. Huang, *J. Mater. Chem.*, 2010, **20**, 5251–5259.
36 F. Grandjean, L. Samain and G. J. Long, *Dalton Trans.*, 2016, **45**, 18018–18044.
37 M. Cao, X. Wu, X. He and C. Hu, *Chem. Commun.*, 2005, 2241–2243, DOI: **10.1039/b500153f**.
38 R. McHale, Y. Liu, N. Ghasdian, N. S. Hondow, S. Ye, Y. Lu, R. Brydson and X. Wang, *Nanoscale*, 2011, **3**, 3685–3694.
39 G. Tartaro, H. Mateos, D. Schirone, R. Angelico and G. Palazzo, *Nanomaterials*, 2020, **10**, 3685–3694.
40 G. Liang, J. Xu and X. Wang, *J. Am. Chem. Soc.*, 2009, **131**, 5378–5379.
41 R. McHale, N. Ghasdian, Y. Liu, M. B. Ward, N. S. Hondow, H. Wang, Y. Miao, R. Brydson and X. Wang, *Chem. Commun.*, 2010, **46**, 4574–4576.
42 R. McHale, N. Ghasdian, Y. Liu, H. Wang, Y. Miao and X. Wang, *Macromol. Rapid Commun.*, 2010, **31**, 856–860.
43 D. Li, M. Liu, W. Li, Q. Fu, L. Wang, E. Lai, W. Zhao and K. Zhang, *Pharmaceuticals*, 2022, **15**, 769.
44 J. Liu, D. Li, K. Zhang, M. Yang, H. Sun and B. Yang, *Small*, 2018, **14**, e1703919.
45 F. Yang, M. Du, K. Yin, Z. Qiu, J. Zhao, C. Liu, G. Zhang, Y. Gao and H. Pang, *Small*, 2021, **18**, 2105715.
46 S. Zhang, Y. Zhang, F. Baig and T.-F. Liu, *Cryst. Growth Des.*, 2021, **21**, 3100–3122.
47 J. Zhai, Y. Zhai, L. Wang and S. Dong, *Inorg. Chem.*, 2008, **47**, 7071–7073.
48 Q. Pan, K. Huang, S. Ni, F. Yang and D. He, *Mater. Res. Bull.*, 2009, **44**, 388–392.
49 F. Yang, S. Hu, Y. Zhang, X. Cai, Y. Huang, F. Wang, S. Wen, G. Teng and N. Gu, *Adv. Mater.*, 2012, **24**, 5205–5211.
50 W. Zhang, S. Hu, J. J. Yin, W. He, W. Lu, M. Ma, N. Gu and Y. Zhang, *J. Am. Chem. Soc.*, 2016, **138**, 5860–5865.
51 Y. Wang, Z. Gong, Y. Zeng, H. Zhao and J. Yang, *Chem. Eng. J.*, 2022, **431**, 2106723.
52 H. Lv, H. Qin, K. Ariga, Y. Yamauchi and B. Liu, *Angew. Chem., Int. Ed.*, 2022, **61**, e202116179.
53 J. Li, H. Huang, X. Cao, H.-H. Wu, K. Pan, Q. Zhang, N. Wu and X. Liu, *Chem. Eng. J.*, 2021, **416**, 127677.
54 F. Feng, S. Chen, X. Z. Liao and Z. F. Ma, *Small Methods*, 2018, **3**, 1800259.
55 X. Han, S. Lin, Y. Li, C. Cheng and X. Han, *Anal. Chim. Acta*, 2020, **1098**, 117–124.
56 J. Domínguez-Vera and E. Colacio, *Inorg. Chem.*, 2003, **42**, 6983–6985.
57 L. Wu, T. Pang, L. Wu, Y. Guan, L. Yin and Y. Li, *J. Inorg. Organomet. Polym. Mater.*, 2020, **30**, 5074–5084.
58 Q. Shen, J. Jiang, M. Fan, S. Liu, L. Wang, Q. Fan and W. Huang, *J. Electroanal. Chem.*, 2014, **712**, 132–138.
59 J. Li, F. Zhang, Z. Hu, W. Song, G. Li, G. Liang, J. Zhou, K. Li, Y. Cao, Z. Luo and K. Cai, *Adv. Healthcare Mater.*, 2017, **6**, 1700005.
60 D. Li, T. Wang, L. Li, L. Zhang, C. Wang and X. Dong, *J. Colloid Interface Sci.*, 2022, **613**, 671–680.
61 S. Wang, M. Qin, M. Huang, X. Huang, Q. Li and Y. You, *ACS Appl. Energy Mater.*, 2022, **5**, 6927–6935.
62 D. Yang, C. A. Gaggioli, D. Ray, M. Babucci, L. Gagliardi and B. C. Gates, *J. Am. Chem. Soc.*, 2020, **142**, 8044–8056.

63 C. Li, X. J. Li, Z. Y. Zhao, F. L. Li, J. Y. Xue, Z. Niu, H. W. Gu, P. Braunstein and J. P. Lang, *Nanoscale*, 2020, **12**, 14004–14010.
64 W. Geng, Z. Zhang, Z. Yang, H. Tang and G. He, *Chem. Commun.*, 2022, **58**, 4472–4475.
65 J. Nai, Y. Lu and X.-Y. Yu, *J. Mater. Chem. A*, 2018, **6**, 21891–21895.
66 Z. Qin, B. Chen, Y. Mao, C. Shi, Y. Li, X. Huang, F. Yang and N. Gu, *ACS Appl. Mater. Interfaces*, 2020, **12**, 57382–57390.
67 D. Zuo, C. Wang, J. Han, J. Wu, H. Qiu, Q. Zhang, Y. Lu, Y. Lin and X. Liu, *ACS Sustainable Chem. Eng.*, 2020, **8**, 16229–16240.
68 X. Wang and L. Cheng, *Coord. Chem. Rev.*, 2020, **419**, 213393.
69 H. Ming, N. L. K. Torad, Y.-D. Chiang, K. C. W. Wu and Y. Yamauchi, *CrystEngComm*, 2012, **14**, 3387.
70 X. Wu, M. Cao, C. Hu and X. He, *Crystal Growth Des.*, 2006, **6**, 26–28.
71 O. Stefanczyk, T. Korzeniak, W. Nitek, M. Rams and B. Sieklucka, *Inorg. Chem.*, 2011, **50**, 8808–8816.
72 Z. Qin, B. Chen, X. Huang, Y. Mao, Y. Li, F. Yang and N. Gu, *Dalton Trans.*, 2019, **48**, 17169–17173.
73 X. Zhang, Q. Qu, W. Cheng, A. Zhou, Y. Deng, W. Ma, M. Zhu, R. Xiong and C. Huang, *Int. J. Biol. Macromol.*, 2022, **209**, 794–800.
74 X. Zhu, H. Tao and M. Li, *Int. J. Hydrogen Energy*, 2020, **45**, 14452–14460.
75 M. B. Zakaria and T. Chikyow, *Coord. Chem. Rev.*, 2017, **352**, 328–345.
76 X. Yang, L. Kang, Z. Wei, S. Lou, F. Lei, P. Hao, J. Xie and B. Tang, *Chem. Eng. J.*, 2021, **422**, 14452–14460.
77 Y. Shang, X. Li, J. Song, S. Huang, Z. Yang, Z. J. Xu and H. Y. Yang, *Chem*, 2020, **6**, 1804–1818.
78 Y. Yue, Z. Zhang, A. J. Binder, J. Chen, X. Jin, S. H. Overbury and S. Dai, *ChemSusChem*, 2015, **8**, 177–183.
79 B. Singh and A. Indra, *Mater. Today Energy*, 2020, **16**, 100404.
80 D. Li, C. Liu, W. Ma, S. Xu, Y. Lu, W. Wei, J. Zhu and D. Jiang, *Electrochim. Acta*, 2021, **367**, 177–183.
81 E. Canto-Aguilar, M. Oliver-Tolentino, G. Ramos-Sánchez and L. González, *Electrochim. Acta*, 2021, **371**, 137828.
82 R. Zhou, P. Wang, Y. Guo, X. Dai, S. Xiao, Z. Fang, R. Speight, E. W. Thompson, P. J. Cullen and K. K. Ostrikov, *Nanoscale*, 2019, **11**, 19497–19505.
83 C. Ma, Z. Jiang, S. Han, Y. Guo, T. Deng and G. Feng, *J. Chem.*, 2021, **2021**, 1–9.
84 J. Huang, P. Xu, T. Gao, J. Huangfu, X.-J. Wang, S. Liu, Y. Zhang and B. Song, *ACS Sustainable Chem. Eng.*, 2019, **8**, 1319–1328.
85 Y. Hao, L. Mao, R. Zhang, X. Liao, M. Yuan and W. Liao, *ACS Appl. Bio Mater.*, 2021, **4**, 7081–7093.
86 X. Jia, M. Lv, Y. Fei, Q. Dong, H. Wang, Q. Liu, D. Li, J. Wang and E. Wang, *Biomaterials*, 2022, **282**, 121404.
87 S. Mukherjee, R. Kotcherlakota, S. Haque, S. Das, S. Nuthi, D. Bhattacharya, K. Madhusudana, S. Chakravarty, R. Sistla and C. R. Patra, *ACS Biomater. Sci. Eng.*, 2020, **6**, 690–704.
88 J. Li, X. Liu, L. Tan, Z. Cui, X. Yang, Y. Liang, Z. Li, S. Zhu, Y. Zheng, K. W. K. Yeung, X. Wang and S. Wu, *Nat. Commun.*, 2019, **10**, 4490.
89 P. Liu, P. Ji, L. Wang, H. Guo, M. Huo and J. Shi, *Biomaterials*, 2022, **289**, 121768.
90 X. Zhao, S. Yao, X. Wan, T. Huang, Z. Zhang, X. Wang, S. Wang, Q. Liang, Z. Li and L. Li, *Appl. Mater. Today*, 2021, **25**, 101255.
91 M. B. Zakaria, C. Li, M. Pramanik, Y. Tsujimoto, M. Hu, V. Malgras, S. Tominaka and Y. Yamauchi, *J. Mater. Chem. A*, 2016, **4**, 9266–9274.
92 X. Cai, W. Gao, L. Zhang, M. Ma, T. Liu, W. Du, Y. Zheng, H. Chen and J. Shi, *ACS Nano*, 2016, **10**, 11115–11126.
93 A. H. Odda, Y. Xu, J. Lin, G. Wang, N. Ullah, A. Zeb, K. Liang, L. P. Wen and A. W. Xu, *J. Mater. Chem. B*, 2019, **7**, 2032–2042.
94 Z. Qin, Y. Li and N. Gu, *Adv. Healthcare Mater.*, 2018, **7**, e1800347.
95 S. Phadke, R. Mysyk and M. Anouti, *J. Energy Chem.*, 2020, **40**, 31–38.
96 Y. Jiang, Y. Yang, L. Shen, J. Ma, H. Ma and N. Zhu, *Anal. Chem.*, 2022, **94**, 297–311.
97 R. Chen, Y. Huang, M. Xie, Q. Zhang, X. Zhang, L. Li and F. Wu, *ACS Appl. Mater. Interfaces*, 2016, **8**, 16078–16086.
98 C. Q. X. Lim, T. Wang, E. W. Y. Ong and Z. K. Tan, *Adv. Mater. Interfaces*, 2020, **7**, 2000853.
99 J. Wang, B. Zhang, J. Sun, W. Hu and H. Wang, *Nano Today*, 2021, **38**, 4472–4475.
100 Y. Li, Z. Jin and N. Tsubaki, *J. Mater. Chem. C*, 2022, 18213–18225.
101 Y. Gao, G. Yu, K. Xing, D. Gorin, Y. Kotelevtsev, W. Tong and Z. Mao, *J. Mater. Chem. B*, 2020, **8**, 7121–7134.
102 X. Y. Yu, L. Yu, H. B. Wu and X. W. Lou, *Angew. Chem., Int. Ed. Engl.*, 2015, **54**, 5331–5335.
103 M. Wang, J. Zhong, Z. Zhu, A. Gao, F. Yi, J. Ling, J. Hao and D. Shu, *J. Alloys Compd.*, 2022, **893**, 162344.
104 Q. Jia, F. Su, Z. Li, X. Huang, L. He, M. Wang, Z. Zhang, S. Fang and N. Zhou, *ACS Appl. Bio Mater.*, 2019, **2**, 2143–2154.
105 X. Hu, X. Wang, X. Hu, C. Xie and D. Zeng, *Chem. Commun.*, 2019, **55**, 13386–13389.
106 X. Cai, X. Jia, W. Gao, K. Zhang, M. Ma, S. Wang, Y. Zheng, J. Shi and H. Chen, *Adv. Funct. Mater.*, 2015, **25**, 2520–2529.
107 J. Chen, F. Xue, W. Du, H. Yu, Z. Yang, Q. Du and H. Chen, *Nano Lett.*, 2022, **22**, 6156–6165.
108 Z. Meng, X. Zhang, H. Tan and H. Lian, *Chem. Eng. J.*, 2022, **435**, 134781.
109 H. Bai, Q. Sun, F. Kong, H. Dong, M. Ma, F. Liu, C. Wang, H. Xu, N. Gu and Y. Zhang, *J. Mater. Chem. B*, 2021, **9**, 5245–5254.
110 W. Chen, K. Zeng, H. Liu, J. Ouyang, L. Wang, Y. Liu, H. Wang, L. Deng and Y.-N. Liu, *Adv. Funct. Mater.*, 2017, **27**, 1605795.
111 R. Yang, M. Hou, Y. Gao, L. Zhang, Z. Xu, Y. Kang and P. Xue, *Nanoscale*, 2019, **11**, 5717–5731.
112 Y. Li, Y. Zhu, C. Wang, Y. Shen, L. Liu, S. Zhou, P. F. Cui, H. Hu, P. Jiang, X. Ni, L. Qiu and J. Wang, *Mol. Pharm.*, 2022, **19**, 819–830.

113 H. Xiong, Y. Zhao, Q. Xu, X. Xie, J. Wu, B. Hu, S. Chen, X. Cai, Y. Zheng and C. Fan, *Small*, 2022, **18**, 2200787.
114 P. Zhang, D. Luan and X. W. D. Lou, *Adv. Mater.*, 2020, **32**, e2004561.
115 K. Zhang, M. Tu, W. Gao, X. Cai, F. Song, Z. Chen, Q. Zhang, J. Wang, C. Jin, J. Shi, X. Yang, Y. Zhu, W. Gu, B. Hu, Y. Zheng, H. Zhang and M. Tian, *Nano Lett.*, 2019, **19**, 2812–2823.
116 X. Jia, X. Cai, Y. Chen, S. Wang, H. Xu, K. Zhang, M. Ma, H. Wu, J. Shi and H. Chen, *ACS Appl. Mater. Interfaces*, 2015, **7**, 4579–4588.
117 P. Singh, S. Kachhap, P. Singh and S. K. Singh, *Coord. Chem. Rev.*, 2022, **472**, 4579–4588.
118 S. Mehta, A. Suresh, Y. Nayak, R. Narayan and U. Y. Nayak, *Coord. Chem. Rev.*, 2022, **460**, 214482.
119 X. Zhang, C. Sui, J. Gong, R. Yang, Y. Luo and L. Qu, *Appl. Surf. Sci.*, 2007, **253**, 9030–9034.
120 M. Hu, J.-S. Jiang, C.-C. Lin and Y. Zeng, *CrystEngComm*, 2010, **12**, 2679–2683.
121 V. Hornok and I. Dekany, *J. Colloid Interface Sci.*, 2007, **309**, 176–182.
122 Y. Gong, Y. Xu, Y. Que, X. Xu, Y. Tang, D. Ye, H. Zhao and J. Zhang, *J. Colloid Interface Sci.*, 2022, **612**, 639–649.
123 X. Zheng, Q. Kuang, T. Xu, Z. Jiang, S. Zhang, Z. Xie, R. Huang and L. Zheng, *J. Phys. Chem. C*, 2007, **111**, 4499–4502.
124 X. Sun, H. Qi, S. Mao and Z. Sun, *Chem. Eng. J.*, 2021, **423**, 130169.
125 D. Ye, M. Li, K. Feng, Y. Zhang, J. Sheng and N. Gu, *Nano Today*, 2022, **44**, 101506.
126 W. P. Li, C. H. Su, L. C. Tsao, C. T. Chang, Y. P. Hsu and C. S. Yeh, *ACS Nano*, 2016, **10**, 11027–11036.
127 F. Shiba, *Colloids Surf., A*, 2010, **366**, 178–182.
128 L. Cheng, H. Gong, W. Zhu, J. Liu, X. Wang, G. Liu and Z. Liu, *Biomaterials*, 2014, **35**, 9844–9852.
129 G. Liang, X. Li, B. Fei, X. Wang and F. Zhu, *Polym. Chem.*, 2015, **6**, 7179–7187.
130 H. Chen, Y. Ma, X. Wang, X. Wu and Z. Zha, *RSC Adv.*, 2017, **7**, 248–255.
131 X. Wang, A. Dong, Z. Zhu, L. Chai, J. Ding, L. Zhong, T. T. Li, Y. Hu, J. Qian and S. Huang, *Small*, 2020, **16**, e2004614.
132 Q. Chen, L. Zhang, L. Li, M. Tan, W. Liu, S. Liu, Z. Xie, W. Zhang, Z. Wang, Y. Cao, T. Shang and H. Ran, *J. Nanobiotechnol.*, 2021, **19**, 449.
133 K. P. Kubelick and S. Y. Emelianov, *Photoacoustics*, 2020, **18**, 100166.
134 H. Wang, R. Qu, Q. Chen, T. Zhang, X. Chen, B. Wu and T. Chen, *J. Mater. Chem. B*, 2022, **10**, 5410–5421.
135 H. Oh, D. Son, J. S. Lee, M. Kim, D. Sung, H. Lee and W. I. Choi, *Int. J. Biol. Macromol.*, 2022, **219**, 835–843.
136 W. Yu, X. Li, Y. Huang, Y. Chen, Q. Gao, Y. Wang and J. Ji, *Biomater. Sci.*, 2021, **9**, 4737–4745.
137 W. Zhang, C. Wang, L. Guan, M. Peng, K. Li and Y. Lin, *J. Mater. Chem. B*, 2019, **7**, 7704–7712.
138 L. Zhang, A. Zhang, D. Du and Y. Lin, *Nanoscale*, 2012, **4**, 4674–4679.
139 E. Mamontova, M. Rodríguez-Castillo, E. Oliviero, Y. Guari, J. Larionova, M. Monge and J. Long, *Inorg. Chem. Front.*, 2021, **8**, 2248–2260.
140 H. Bae, T. Ahmad, I. Rhee, Y. Chang, S. Jin and S. Hong, *Nanoscale Res. Lett.*, 2012, **7**, 1–5.
141 P. R. Sajanlal, T. S. Sreeprasad, A. K. Samal and T. Pradeep, *Nano Rev.*, 2011, **2**, 5883.
142 A. I. Lopez-Lorente, *Anal. Chim. Acta*, 2021, **1168**, 338474.
143 K. Zhang, Z. Zhang, X. Zhou and N. Zhang, *Electroanalysis*, 2021, **33**, 1167–1174.
144 L. Jing, X. Liang, Z. Deng, S. Feng, X. Li, M. Huang, C. Li and Z. Dai, *Biomaterials*, 2014, **35**, 5814–5821.
145 Y. Wang, X. Pang, J. Wang, Y. Cheng, Y. Song, Q. Sun, Q. You, F. Tan, J. Li and N. Li, *J. Mater. Chem. B*, 2018, **6**, 2460–2473.
146 X. Mei, Y. Han, J. Xi, J. Liu, L. Xu, J. Yuan, S. Wang, X. Li, W. Si and J. Li, *Mater. Lett.*, 2022, **312**, 131697.
147 Y. N. Wang, W. S. Zhang, X. P. Liu, Y. Y. Wei and Z. R. Xu, *Colloids Surf., B*, 2022, **215**, 112490.
148 D. Zhong, Y. Wang, F. Xie, S. Chen, X. Yang, Z. Ma, S. Wang, M. Z. Iqbal, J. Ge, Q. Zhang, R. Zhao and X. Kong, *J. Mater. Chem. B*, 2022, **10**, 4889–4896.
149 J. Cao, W. Zhu, A. G. Shen and J. M. Hu, *J. Colloid Interface Sci.*, 2022, **610**, 621–633.
150 J. Wang, M. Zhang, J. Li, F. Jiao, Y. Lin and Y. Gong, *Dalton Trans.*, 2020, **49**, 14290–14296.
151 M. Xu, B. Chi, Z. Han, Y. He, F. Tian, Z. Xu, L. Li and J. Wang, *Dalton Trans.*, 2020, **49**, 12327–12337.
152 Y. Luo, J. Li, X. Liu, L. Tan, Z. Cui, X. Feng, X. Yang, Y. Liang, Z. Li, S. Zhu, Y. Zheng, K. W. K. Yeung, C. Yang, X. Wang and S. Wu, *ACS Cent. Sci.*, 2019, **5**, 1591–1601.
153 Z. Hu, S. Wang, Z. Dai, H. Zhang and X. Zheng, *J. Mater. Chem. B*, 2020, **8**, 5351–5360.
154 Z. H. Li, Y. Chen, Y. Sun and X. Z. Zhang, *ACS Nano*, 2021, **15**, 5189–5200.
155 E. Zeimaran, S. Pourshahrestani, A. Fathi, N. Razak, N. A. Kadri, A. Sheikhi and F. Baino, *Acta Biomater.*, 2021, **136**, 1–36.
156 W. Xu, Y. Zhang, Y. Gao and M. J. Serpe, *ACS Appl. Mater. Interfaces*, 2018, **10**, 13124–13129.
157 Z. Li, W. Xu, J. Yang, J. Wang, J. Wang, G. Zhu, D. Li, J. Ding and T. Sun, *Adv. Mater.*, 2022, **34**, e2200449.
158 H. Zhang, X. Sun, J. Wang, Y. Zhang, M. Dong, T. Bu, L. Li, Y. Liu and L. Wang, *Adv. Funct. Mater.*, 2021, **31**, 2100093.
159 C. Yu, X. Liu, J. Zhang, Y. Chao, X. Jia, C. Wang and G. G. Wallace, *Small Methods*, 2022, **6**, e2200344.
160 X. Song, X. Wang, J. Zhang, S. Shen, W. Yin, G. Ye, L. Wang, H. Hou and X. Qiu, *Biomaterials*, 2021, **273**, 120811.
161 X. Liu, Q. Zhang and G. Gao, *Chem. Eng. J.*, 2020, **394**, 2200344.
162 M. Borzenkov, L. D'Alfonso, A. Polissi, P. Sperandeo, M. Collini, G. Dacarro, A. Taglietti, G. Chirico and P. Pallavicini, *Nanotechnology*, 2019, **30**, 295702.
163 C. Xu, D. Jiang, Y. Ge, L. Huang, Y. Xiao, X. Ren, X. Liu, Q. Zhang and Y. Wang, *Chem. Eng. J.*, 2022, **431**, 134109.
164 J. Fu, B. Wu, M. Wei, Y. Huang, Y. Zhou, Q. Zhang and L. Du, *Acta Pharm. Sin. B*, 2019, **9**, 604–614.

165 Z. Chen, R. Chen, C. Zhao, Z. Quan, H. Zhu, L. Wang, Q. Bu, Y. He and H. He, *Chem. Eng. J.*, 2022, **431**, 133255.
166 D. Zhu, Z. Zheng, G. Luo, M. Suo, X. Li, Y. Duo and B. Z. Tang, *Nano Today*, 2021, **37**, 101091.
167 Z. Xu, Y. Liu, R. Ma, J. Chen, J. Qiu, S. Du, C. Li, Z. Wu, X. Yang, Z. Chen and T. Chen, *ACS Appl. Mater. Interfaces*, 2022, **14**, 14059–14071.
168 E. Cho, J. Kim, C. W. Park, K. W. Lee and T. S. Lee, *J. Hazard. Mater.*, 2018, **360**, 243–249.
169 D. Oh, B. Kim, S. Kang, Y. Kim, S. Yoo, S. Kim, Y. Chung, S. Choung, J. Han, S. Jung, H. Kim and Y. Hwang, *Sci. Rep.*, 2019, **9**, 16334.
170 M. Cheng, W. Peng, P. Hua, Z. Chen, J. Sheng, J. Yang and Y. Wu, *RSC Adv.*, 2017, **7**, 18270–18276.